Self-Assembly and Anion Encapsulation Properties of Cavitand-Based Coordination Cages

Federica Fochi,[†] Paola Jacopozzi,[†] Elina Wegelius,[‡] Kari Rissanen,[‡] Pietro Cozzini,[§] Elena Marastoni,[†] Emilia Fisicaro,[⊥] Paola Manini,[∥] Roel Fokkens,[&] and Enrico Dalcanale*[,†]

Contribution from the Dipartimento di Chimica Organica e Industriale, Università di Parma, Parco Area delle Scienze 17/A, I-43100 Parma, Italy, Laboratory of Organic Chemistry, University of Jyväskylä, P.O. Box 35, FIN-40351 Jyväskylä, Finland, Dipartimento di Chimica Generale ed Inorganica, Chimica Analitica, Chimica Fisica, Università di Parma, Parco Area delle Scienze 17/A, I-43100 Parma, Italy, Dipartimento Farmaceutico, Università di Parma, Parco Area delle Scienze 27/A, I-43100 Parma, Italy, Dipartimento di Clinica Medica, Nefrologia e Scienze della Prevenzione, Università di Parma, Via Gramsci 14, I-43100 Parma, Italy, and Laboratory of Supramolecular Chemistry and Technology, MESA+ Research Institute, University of Twente, P.O. Box 217, 7500 AE Enschede, The Netherlands

Received February 7, 2001

Abstract: Two novel classes of cavitand-based coordination cages **7a**−**j** and **8a**−**d** have been synthesized via self-assembly procedures. The main factors controlling cage self-assembly (CSA) have been identified in (i) a P−M−P angle close to 90° between the chelating ligand and the metal precursor, (ii) Pd and Pt as metal centers, (iii) a weakly coordinated counterion, and (iv) preorganization of the tetradentate cavitand ligand. Calorimetric measurements and dynamic ^{1}H and ^{19}F NMR experiments indicated that CSA is entropy driven. The temperature range of the equilibrium cage-oligomers is determined by the level of preorganization of the cavitand component. The crystal structure of cage **7d** revealed the presence of a single triflate anion encapsulated. Guest competition experiments revealed that the encapsulation preference of cages **7b**,**d** follows the order $BF_4^- > CF_3SO_3^- \gg PF_6^-$ at 300 K. ES-MS experiments coupled to molecular modeling provided a rationale for the observed encapsulation selectivities. The basic selectivity pattern, which follows the solvation enthalpy of the guests, is altered by size and shape of the cavity, allowing the entrance of an ancillary solvent molecule only in the case of BF_4^-.

Introduction

Container molecules are unique among synthetic molecular receptors because of their peculiar encapsulation properties.[1] A wide range of guests of different size, shape, and charge have been trapped within their interior in a time scale which can span from microseconds to forever. Desired features of container molecules comprise selectivity in guest encapsulation, control of guest orientation and dynamics within the cage, and reversibility, which allows guest uptake and release under controlled conditions. Equipped with such features, many potential applications can be envisioned for molecular containers, ranging from specific drug release to catalysis[2] and memory storage devices.[3]

The central issue of their preparation has been tackled both via covalent synthesis and, more recently, via self-assembly.[4] In particular, metal-directed self-assembly is emerging as one of the most promising approaches to the generation of complex supramolecular architectures, due to the large number of coordination motifs and multidentate ligands available. Molecules with a wide variety of topologies and shapes have been constructed in this way, including boxes, cages, catenanes, dendrimers, grids, helicates, rotaxanes, and others.[5] Multidentate pyridine ligands[6] are the most popular building blocks for metal-assembled molecular containers, followed by cathecolates[7] and others.[8] Cavitand-based coordination cages are receiving in-

* Corresponding author. Fax +39-0521-905472. E-mail: enrico.dalcanale@unipr.it.

[†] Dipartimento di Chimica Organica e Industriale, Università di Parma.

[‡] University of Jyväskylä.

[§] Dipartimento di Chimica Generale ed Inorganica, Chimica Analitica, Chimica Fisica, Università di Parma.

[⊥] Dipartimento Farmaceutico, Università di Parma.

[∥] Dipartimento di Clinica Medica, Nefrologia e Scienze della Prevenzione, Università di Parma.

[&] University of Twente.

(1) (a) Cram, D. J.; Cram, J. M. *Container Molecules and their Guests, Monographs in Supramolecular Chemistry*; Stoddart, J. F., Ed.; Royal Society of Chemistry: Cambridge, 1994; Vol. 4. (b) Sherman, J. C. *Tetrahedron* **1995**, *51*, 3395−3422. (c) Rebek, J., Jr. *Chem. Soc. Rev.* **1996**, 255−264. (d) Warmuth, R. *J. Inclusion Phenom. Mol. Recognit. Chem.* **2000**, *37*, 1−38.

(2) Kang, J.; Hilmersson, G.; Santamaría, J.; Rebek, J., Jr. *J. Am. Chem. Soc.* **1998**, *120*, 3650−3656.

(3) van Wageningen, A. M. A.; Timmerman, P.; van Duynhoven, J. P. M.; Verboom, W.; van Veggel, F. C. J. M.; Reinhoudt, D. N. *Chem. Eur. J.* **1997**, *3*, 639−654.

(4) (a) Conn, M. M.; Rebek, J., Jr. *Chem. Rev.* **1997**, *97*, 1647−1668. (b) MacGillivray, L. R.; Atwood, J. L. *Angew. Chem., Int. Ed.* **1999**, *38*, 1018−1033. (c) Jasat, A.; Sherman, J. C. *Chem. Rev.* **1999**, *99*, 931−967.

(5) For recent reviews on this topic, see: (a) Lehn, J.-M. *Supramolecular Chemistry: Concepts and Perspectives*; VCH: Weinheim, Germany, 1995; pp 144−160. (b) Baxter, P. N. W. In *Comprehensive Supramolecular Chemistry*; Lehn, J.-M., Chair Ed.; Atwood, J. L., Davis, J. E. D., MacNicol, D. D., Vogtle, F., Executive Eds.; Pergamon Press: Oxford, U.K., 1996; Vol. 9, Chapter 5, pp 165−211. (c) Fujita, M. In *Comprehensive Supramolecular Chemistry*; Lehn, J.-M., Chair Ed.; Atwood, J. L., Davis, J. E. D., MacNicol, D. D., Vogtle, F., Executive Eds.; Pergamon Press: Oxford, U.K., 1996; Vol. 9, Chapter 7, pp 253−282. (d) Fujita, M. *Chem. Soc. Rev.* **1999**, *27*, 417−425. (e) Caulder, D. L.; Raymond, K. N. *Acc. Chem. Res.* **1999**, *32*, 975−982. (f) Saalfrank, R. W.; Demleitner, B. In *Transition Metals in Supramolecular Chemistry; Perspectives in Supramolecular Chemistry;* Sauvage, J. P., Ed.; Wiley-VCH: Weinheim, 1999, Vol. 5, pp 1−51. (g) Leininger, S.; Olenyuk, B.; Stang, P. J. *Chem. Rev.* **2000**, *100*, 853−908.

10.1021/ja0103492 CCC: $20.00
Published on Web 07/13/2001

Chart 1

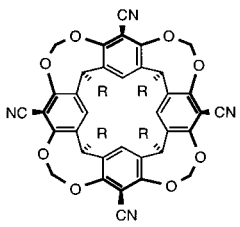

1a R=C_6H_{13}
1b R=$C_{11}H_{23}$
1c R=CH_2CH_2Ph

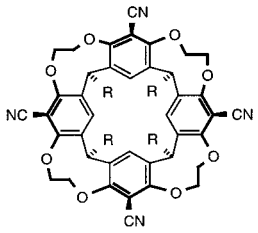

2a R=C_6H_{13}
2b R=$C_{11}H_{23}$

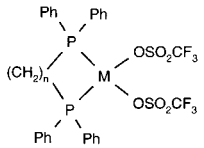

3a M=Pd n=1
3b M=Ni n=2
3c M=Pd n=2
3d M=Pt n=2
3e M=Ni n=3
3f M=Pd n=3
3g M=Pt n=3
3h M=Pd n=4

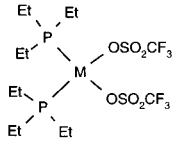

4a M=Pt

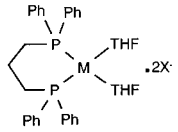

5a M=Pd X=BF_4^-
5b M=Pt X=BF_4^-
5c M=Pd X=PF_6^-
5d M=Pt X=PF_6^-

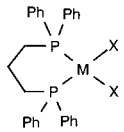

6a M=Pd X=CF_3COO^-
6b M=Pt X=CF_3COO^-
6c M=Pd X=OTs^-
6d M=Pd X=CH_3COO^-

creasing attention[9] due to the versatility of cavitand platforms in terms of synthetic modularity and molecular recognition phenomena. In all cases they have been employed as tetradentate ligands by introducing four ligand moieties at the upper rim.

In a previous communication we reported the metal-directed self-assembly of new cavitand-based coordination cages in which two tetracyano cavitands are connected through four Pd^{II} or Pt^{II} square-planar complexes.[9a] Here we present (i) preparation and characterization of a whole family of cages, including the X-ray crystal structure of one of them, (ii) the factors controlling the self-assembly process in terms of metal, chelating ligand, counterion, geometry, and preorganization of the molecular components, (iii) evidences that the self-assembly process is entropy driven, (iv) self-selection of the cavitand components, and (v) the anion encapsulation properties of the cages.

Results and Discussion

Synthesis of the Molecular Components (Chart 1). Tetracyano cavitands **1a**−**c** and **2a**,**b** were prepared from the corresponding tetrabromo cavitands using the Rosenmund−von Brown reaction (see Experimental Section). Cavitands **1a**−**c** are conformationally rigid (C_{4v}-cone symmetry) with the four nitriles preorganized in a fixed, diverging spatial orientation. The presence of four ethylene bridges in cavitands **2a**,**b** imparts a limited degree of conformational mobility which, in solution, allows **2a**,**b** to rapidly interconvert between two equivalent flattened cone conformations.[10] Upon cooling to 223 K in CD_2Cl_2, no splitting of the proton signals was observed for **2a**,**b**, indicating that the interconversion between the two flattened cone C_{2v} conformers through the C_{4v} symmetry cone conformer, in which all four nitriles have the same angle with respect to the C_4 axis, is fast in the temperature range of cage formation.

Square-planar *cis*-metal bis(triflate) complexes **3a**−**g** and **4a** were prepared via chelation of the corresponding MCl_2 salt, followed by exchange of the anionic ligands with AgOTf (OTf = triflate) in CH_2Cl_2. In the case of Pd(dppb)$(OTf)_2$ **3h**, ligand substitution of $Pd(C_6H_5CN)_2Cl_2$ with dppb[11] was required to afford the complex Pd(dppb)Cl_2, followed by reaction with AgOTf. M(dppp)X_2 complexes **5a**−**d** and **6a**−**c** were obtained via ligand exchange of M(dppp)Cl_2 with the corresponding AgX salts, while Pd(dppp)$(CH_3COO)_2$ **6d** was formed by reaction of palladium acetate with dppp. Platinum complexes **5b** and **5d** are stable only in THF solution and were used immediately after their preparation.

Self-Assembly and Characterization of the Coordination Cages. The typical procedure for cage formation is shown in the case of cavitand **1a**−**c** and metal precursors **3f**−**g** (Scheme 1): by mixing the two components in a 1:2 molar ratio at room temperature in solvents such as CH_2Cl_2, $CHCl_3$, or acetone cages **7a**−**e** were obtained in quantitative yield. Cages **7a**−**d** were recovered in pure form by simple evaporation of the solvent,

(6) For recent examples of molecular containers assembled using multidentate pyridine ligands, see: (a) Takeda, N.; Umemoto, K.; Yamaguchi, K.; Fujita, M. *Nature* **1999**, *398*, 794−796. (b) Olenyuk, B.; Whiteford, J. A.; Fechtenkötter, A.; Stang, P. J. *Nature* **1999**, *398*, 796−799. (c) Kusukawa, T.; Fujita, M. *J. Am. Chem. Soc.* **1999**, *121*, 1397−1398. (d) Ikeda, A.; Yoshima, M.; Udzu, H.; Fukuhara, C.; Shinkai, S. *J. Am. Chem. Soc.* **1999**, *121*, 4296−4297. (e) Hiraoka, S.; Fujita, M. *J. Am. Chem. Soc.* **1999**, *121*, 10239−10240. (f) Olenyuk, B.; Levin, M. D.; Whiteford, J. A.; Shield, J. E.; Stang, P. J. *J. Am. Chem. Soc.* **1999**, *121*, 10434−10435.

(7) For molecular containers assembled using multidentate cathecolate ligands, see ref 5e.

(8) For miscellaneous ligands, see: (a) Saalfrank, R. W.; Burak, R.; Breit, A.; Stalke, D.; Herbst-Irmer, R.; Daub, J.; Porsch, M.; Bill, E.; Müther, M.; Trautwein, A. X. *Angew. Chem., Int. Ed. Engl.* **1994**, *33*, 1621−1623. (b) Mann, S.; Huttner, G.; Zsolnai, L.; Heinze, K. *Angew. Chem., Int. Ed. Engl.* **1996**, *35*, 2808−2809. (c) Saalfrank, R. W.; Bernt, I.; Uller, E.; Hampel, F. *Angew. Chem., Int. Ed. Engl.* **1997**, *36*, 2482−2485. (d) Hartshorn, C. M.; Steel, P. J. *Chem. Commun.* **1997**, 541−542. (e) Lee, S. B.; Hong, J.-I. *Tetrahedron Lett.* **1998**, *39*, 4317−4320. (f) Abrahams, B. F.; Egan, S. J.; Robson, R. *J. Am. Chem. Soc.* **1999**, *121*, 3535−3536.

(9) (a) Jacopozzi, P.; Dalcanale, E. *Angew. Chem., Int. Ed. Engl.* **1997**, *36*, 613−615. (b) Fox, D. O.; Dalley, N. K.; Harrison, R. G. *J. Am. Chem. Soc.* **1998**, *120*, 7111−7112. (c) Fox, O. D.; Drew, M. G. B.; Beer, P. D. *Angew. Chem., Int. Ed.* **2000**, *39*, 136−140. (d) Cuminetti, N.; Ebbing, M. H. K.; Prados, P.; de Mendoza, J.; Dalcanale, E. *Tetrahedron Lett.* **2001**, *42*, 527−530.

(10) Cram, D. J.; Karbach, S.; Kim, H.-E.; Knobler, C. B.; Maverick, E. F.; Ericson, J. L.; Helgeson, R. C. *J. Am. Chem. Soc.* **1988**, *110*, 2229−2237.

(11) Ligand abbreviations: dppm = bis(diphenylphosphino)methane; dppe = 1,2-bis(diphenylphosphino)ethane; dppp = 1,3-bis(diphenylphosphino)propane; dppb = 1,4-bis(diphenylphosphino)butane.

Scheme 1

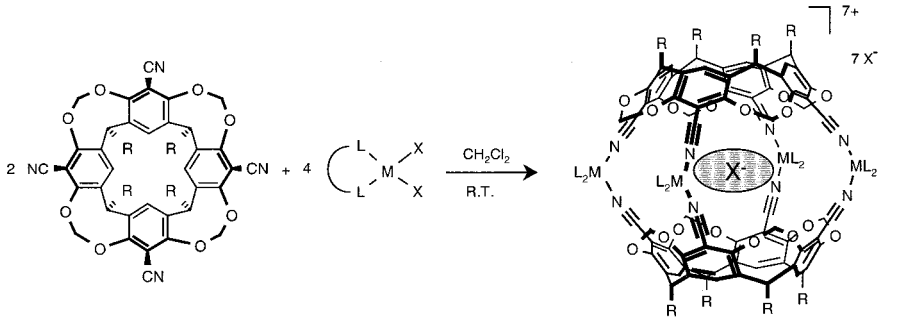

1a-c **3a-h** **4a** **5a-d** **6a-d**

7a	$R=C_6H_{13}$	M=Pd	L_2=dppp	$X=CF_3SO_3^-$
7b	$R=C_{11}H_{23}$	M=Pd	L_2=dppp	$X=CF_3SO_3^-$
7c	$R=C_6H_{13}$	M=Pt	L_2=dppp	$X=CF_3SO_3^-$
7d	$R=C_{11}H_{23}$	M=Pt	L_2=dppp	$X=CF_3SO_3^-$
7e	$R=CH_2CH_2Ph$	M=Pt	L_2=dppp	$X=CF_3SO_3^-$
7f	$R=C_{11}H_{23}$	M=Pd	L_2=dppb	$X=CF_3SO_3$
7g	$R=C_{11}H_{23}$	M=Pt	$L=PEt_3$	$X=CF_3SO_3^-$
7h	$R=C_{11}H_{23}$	M=Pd	L_2=dppp	$X=BF_4^-$
7i	$R=C_{11}H_{23}$	M=Pt	L_2=dppp	$X=BF_4^-$
7k	$R=C_{11}H_{23}$	M=Pd	L_2=dppp	$X=PF_6^-$
7j	$R=C_{11}H_{23}$	M=Pt	L_2=dppp	$X=PF_6^-$

while **7e** precipitated out of the reaction medium. All cages are stable both in the solid state and in solution and soluble in chlorinated and aromatic solvents. A tetrachloroethane solution of **7b** was kept overnight at 100 °C and then the cage was recovered unchanged.

Their ^{1}H NMR spectra showed the complete absence of absorptions belonging to both precursors and the formation of a new set of signals, indicative of the presence of a single highly symmetric compound (D_{4h} symmetry).[9a] In all cases, upon formation of the cage, upfield shifts were observed for the inner methylene bridge and the methyne protons of the cavitand moiety, while aromatic protons were shifted downfield. The upfield shift of the methyne protons is particularly indicative since it can be attributed to shielding caused by the close proximity of dppp aromatic rings in the formed cage (see crystal structure). The downfield shift of the aromatic protons instead is diagnostic of nitrile coordination to the metal. Likewise the methylene signals of dppp were shifted downfield upon complexation. Nitrile−metal coordination was also demonstrated by FT-IR spectroscopy: the nitrile stretching band of the cages is shifted to higher wavenumbers than that of the free cavitands. The high symmetry of the cages was confirmed by their ^{31}P NMR spectra, which exhibited sharp singlets, with appropriate Pt satellites for Pt complexes **7c**−**e**, indicating the equivalence of the eight dppp phosphorus atoms. The triflate counterions of all cages instead experience two different environments: their ^{19}F NMR spectra exhibited two singlets in a 7:1 integral ratio, the bigger one at about −78 ppm, typical of noncoordinated ionic triflates,[12] and a smaller one shifted upfield at about −82 ppm, indicative of the encapsulation of one triflate anion inside the cage.

Additional evidences for the self-assembly of the cages were obtained by using electrospray mass spectrometry (ES-MS).[13] ES-MS proved to be a powerful technique for the investigation of coordination cages in terms of (i) characterization, (ii) individuation of competitive oligomeric species, and (iii) the presence of solvent molecules trapped within the cages. For **7a**−**e** ES-MS showed prominent $[M - 2CF_3SO_3^-]^{2+}$ and $[M - 3CF_3SO_3^-]^{3+}$ peaks; the molecular ions could not be detected since their molecular weight exceeded the limit of the instrument.

MALDI-TOF spectrometry was carried out on cage **7d** to exclude the presence of species having a different stoichiometry of the components consistent with D_{4h} symmetry, such as wider cages formed by four cavitands and eight organometallic precursors. In agreement with the proposed structure, the $[M - CF_3SO_3^-]^+$ signal at *m*/*z* 5981 is the dominant peak of the spectrum (Supporting Information) and the only one present above 4000 Da. Signals corresponding to different aggregates were not observed in the spectrum.

Suitable crystals of **7d** for X-ray analysis were obtained from a dichloromethane−benzene solvent mixture. Two coordination cages A and B (Figure 1) having slightly different conformations were found in the unit cell. Both cages are filled with a single triflate anion, without any ancillary solvent molecule present. The distances and angles relevant to the shape and coordination geometry are defined in drawing I. The internal cavity resembles an oblate sphere: the long axis *a*, defined as the distance between opposite Pt atoms, is 13.5(1) Å for cage A and 13.7(1) Å for cage B. The short axis *b* is 12.1(1) Å for cage A and 11.9(1) Å for cage B and is defined as the distance between the centroids of the four resorcinarene methine carbons. These distances are in agreement with the dimensions of the cavity calculated using the GRASP program. The included triflate cannot escape from the lateral portals without breaking a coordinative bond.

Platinum metals have slightly distorted square-planar coordination spheres: the angles around Pt range from 87(1) to 92(1)° and from 175(1) to 179(1)°. Moreover, the nitriles are not perfectly aligned in the direction of the Pt metals, the β angles C≡N−Pt being 168(1), 172(1), 168(1), and 166(1)° for cage A and 170(1), 165(1), 169(1), and 170(1)° for cage B. In addition, the nitriles are slightly bent from the aromatic rings toward the Pt metals with C(Ar)−C≡N angles from 174(1) to 179(1)°. The nonideal value of the angle α [30.1(3)° < α <

(12) Lawrence, G. A. *Chem. Rev.* **1986**, *86*, 17−33.

(13) For studies of noncovalent aggregation by ES-MS, see: (a) Marquis-Rigault, A.; Dupont-Gervais, A.; Van Dorsselaer, A.; Lehn, J.-M. *Chem. Eur. J.* **1996**, *2*, 1395−1398. (b) Hirsch, K. A.; Wilson, S. R.; Moore, J. S. *J. Am. Chem. Soc.* **1997**, *119*, 10401−10412. (c) Schalley, C. A.; Martín, T.; Obst, U.; Rebek, J., Jr. *J. Am. Chem. Soc.* **1999**, *121*, 2133-2138.

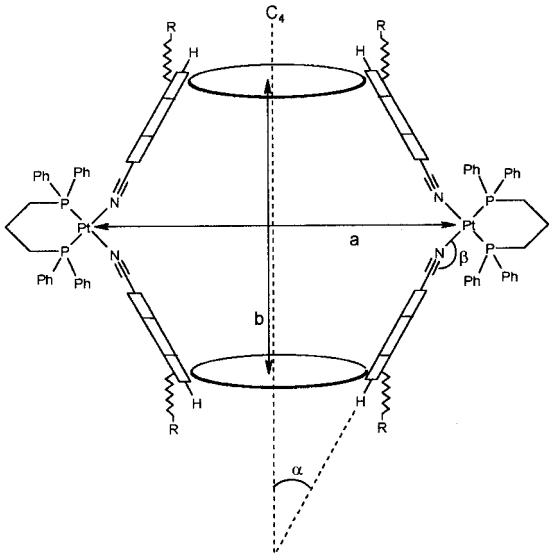

31.4(3)°], imposed by the rigid structure of the cavitand, does not allow the nitriles to assume the most favorable alignment with respect to the Pt atoms. The distances of Pt(II) ions from the best planes through the nitrogen and phosphorus atoms bonded to Pt are 0.03(1), 0.05(1), 0.03(1), and 0.03(1) Å for Pt1, Pt2, Pt3, and Pt4, respectively, indicating nearly no strain in the coordination. The average bond distance of Pt...N is 2.05(1) Å and Pt...P 2.25(1) Å.

Triflate anions included into the cavities are highly disordered between two positions and badly resolved from the X-ray data. In both positions the CF_3 of the triflate points toward the cavitand scaffold. The shortest triflate−resorcinarene distances [F478...C34 = 3.15(4) and F478...C30 = 3.16(3) Å] reveal weak interactions between triflate and the resorcinarene part of cage A. In the case of cage B one triflate fluorine atom interacts strongly with some resorcinarene carbon atoms [F488...C204 = 2.24(3) and F488...C205 = 2.61(3) Å]. The displaced positions of the included anion with respect to the cavity center are due to interactions of the CF_3 moiety of the anion with the cavitand concave surface.

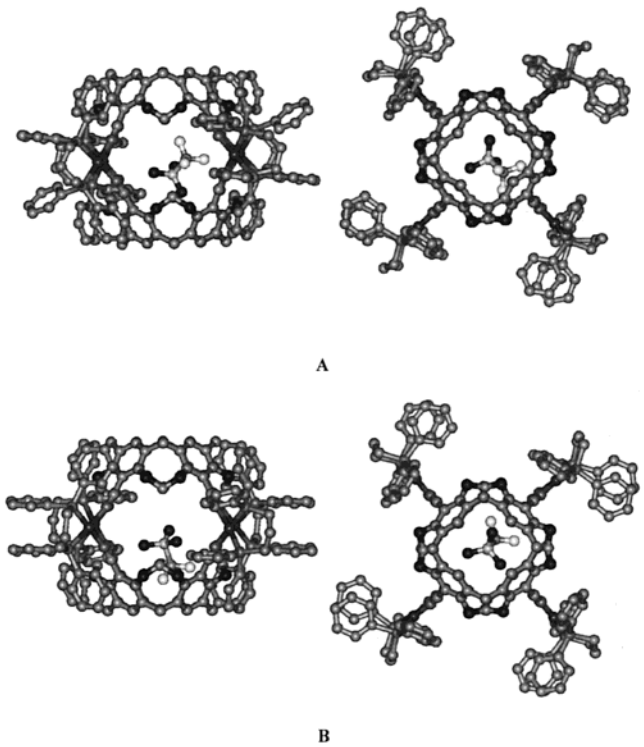

Figure 1. Side and top views of the molecular structure of **7d** showing the two orientations A and B assumed by the included triflate anion. Solvent benzene molecules, alkyl chains of the cavitands, external triflate anions, and hydrogen atoms are omitted for clarity.

Table 1. Cage Self-Assembly (CSA) Using Cavitand **1b** as Tetradentate Ligand and Organometallic Precursors **3a**−**h** and **4a**

entry	organometallic precursor	outcome
1	Pd(dppm)$(OTf)_2$ (**3a**) (72.7°)[a]	no CSA
2	Ni(dppe)$(OTf)_2$ (**3b**) (86.9°)[a]	no CSA
3	Pd(dppe)$(OTf)_2$ (**3c**) (85.8°)[a]	no CSA
4	Pt(dppe)$(OTf)_2$ (**3d**) (85.1°)[a]	oligomers formation at 300 K; partial CSA at 373 K
5	Ni(dppp)$(OTf)_2$ (**3e**)	no CSA
6	Pd(dppp)$(OTf)_2$ (**3f**) (90.6°)[a]	CSA (**7b**)
7	Pt(dppp)$(OTf)_2$ (**3g**) (89.3°)[a]	CSA (**7d**)
8	Pd(dppb)$(OTf)_2$ (**3h**) (97.6°)[a]	partial CSA at 300 K; CSA at 373 K (**7f**)
9	*Cis*-Pt$(PEt_3)_2(OTf)_2$ (**4a**)	partial CSA at 300 K; CSA at 328 K (**7g**)

[a] P−M-P angle of M(dppx)Cl_2 complexes taken from the crystal structures.[15]

In addition to two cages and the included triflate anions, 14 triflate anions and 25 solvent benzene molecules together with folded long alkyl chains of the resorcinarenes fill the interstices of the unit cell.

Control of the Self-Assembly Process. The self-assembly process considered in this work leads to molecular cages via formation of four square-planar transition metal complexes. In every complex two adjacent coordination sites are occupied by nitriles, each belonging to a separate cavitand. The *cis* coordination geometry, a necessary condition for cage self-assembly (CSA), is imposed using dppp as chelating ligand. Therefore, the following structural parameters have been examined as the key factors controlling the self-assembly process: (i) choice of chelating ligand, transition metal, and counterions of the metal precursor, (ii) preorganization and stiffness of the tetradentate cavitand ligand.

The influences of the chelating ligand and of the type of metal have been analyzed by mixing cavitand **1d** with organometallic triflate precursors **3a**−**h** and **4a**, under standard self-assembly conditions. The results are reported in Table 1. All the chosen complexes assume square-planar coordination geometry in solution, except for Ni(dppp)$(OTf)_2$ **3e**, which in solution is in equilibrium between the tetrahedral and square-planar forms.[14] The effect of varying the chelate ring size has been examined in the Pd series (entries 1, 3, 6, and 8). The stepwise increase in the number of carbon atoms of the chelating ligand leads to a progressive widening of the P−Pd−P angle and to a consequent reduction of the CN−Pd−NC angle in the complex (see for comparison the P−M−P angle of the M(dppx)Cl_2 complexes in Table 1 taken from their X-ray crystal structures).[15] The results clearly indicate that the CSA is highly sensitive to distortion from the optimal square-planar arrangement of the four ligands provided by dppp, particularly when the P−M−P angle is smaller than 90°. In fact, in the case of dppb (**3h**, entry 8) partial cage formation was observed at 300 K, which became complete at 373 K (the reasons of this temperature dependence

(14) Van Hecke, G. R.; DeW. Horrocks, W., Jr. *Inorg. Chem.* **1966**, *5*, 1968−1974.

(15) The complete set of X-ray crystal structures is available only for the M(dppx)Cl_2 series (see Steffen, W. L.; Palenik, G. J. *Inorg. Chem.* **1976**, *15*, 2432−2438 and reference cited therein). The reported P−M−P angles have been obtained through the Cambridge Data Bank.

Table 2. Cage Self-Assembly (CSA) Using Cavitand **1b** as Tetradentate Ligand and M(dppp)X_2 **5a**−**d** and **6a**−**d** as Organometallic Precursors

anion	Pd	Pt
$CF_3SO_3^-$ (**3f**−**g**)	CSA (**7b**)	CSA (**7d**)
BF_4^- (**5a**−**b**)	CSA (**7h**)	CSA (**7i**)
PF_6^- (**5c**−**d**)	CSA (**7k**)	CSA (**7j**)
CF_3COO^- (**6a**−**b**)	no CSA	no CSA
TsO^- (**6c**)	no CSA	
CH_3COO^- (**6d**)	no CSA	

will be analyzed in the following paragraph). In the other two cases (entries 1 and 3) the CSA was completely suppressed at any temperature. The X-ray crystal structure of **7d** supports these results, showing almost no strain in the coordination sphere of the four Pt complexes. Likewise, exchange of dppp with dppe in the Pt complexes (compare entries 4 and 7) destabilizes the cage with respect to open oligomers. By comparison, the use of ethylenediamine as chelating ligand in the form of Pt(en)-$(OTf)_2$ totally inhibited CSA, giving no reaction with **1c**. The partial CSA observed in the case of **4a** to give cage **7g** (entry 9) at room temperature demonstrates that the absence of a chelating ligand destabilizes the cage with respect to alternative open species.

The influence of the transition metal has been highlighted in the M(dppe)$(OTf)_2$ and M(dppp)$(OTf)_2$ series (entries 2−7). The observed trend in cavitand nitriles coordination (Pt > Pd > Ni) correlates with the relative strength of the CN−M dative bonds. In the favorable case of dppp as chelating ligand, both Pd and Pt complexes led to the formation of **7b**,**d**, while for dppe only the Pt complex **3d** was able to coordinate to the cavitand nitriles giving rise to open oligomers. The behavior of Ni(dppp)$(OTf)_2$ **3e** is more difficult to rationalize: its reluctance to enter the self-assembly game can be due either to the weakness of the CN−Ni bond or to the presence in solution of the tetrahedral form, which is not compatible with cage formation.

Another basic factor to be considered for CSA is the selection of the counterions, which must be weakly coordinated to the metal precursor in order to allow the exchange with the nitriles of the cavitand ligands. For this reason triflate complexes were selected first. The results of a series of experiments performed on cavitand **1b** with metal precursors M(dppp)X_2 **5a**−**d** and **6a**−**d** are summarized in Table 2. CSA proceeded nicely with noncoordinating counterions such as BF_4^- and PF_6^- but failed with the acetate, trifluoroacetate, and tosylate anions, which are too strongly coordinated to the metal to undergo ligand exchange with the nitriles. To check further this hypothesis, the following experiment was devised (Scheme 2): Tetrabutylammonium trifluoroacetate was added to cages **7b** and **7d** respectively in the correct 8:1 stoichiometric ratio required to replace all nitriles, recording ^{1}H NMR and ^{19}F NMR spectra of the resulting mixtures immediately after the addition of the salt. The ^{1}H NMR spectrum revealed complete cage disassembly with release of the free cavitand **1b**, while the ^{19}F NMR showed the formation of the M(dppp)$(CF_3COO)_2$ complexes **6a**,**b** and of tetrabutylammonium triflate. This experiment clearly indicates that CF_3COO^- anions readily replace the nitriles in the cage metal complexes, therefore inhibiting CSA.

The preorganization of the cavitand ligand is another essential ingredient of the self-assembly recipe. The influence of the

Scheme 2

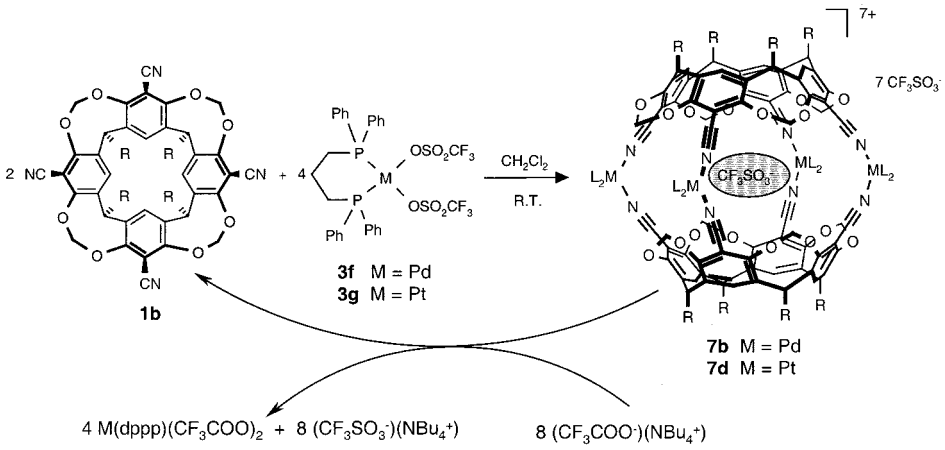

Scheme 3

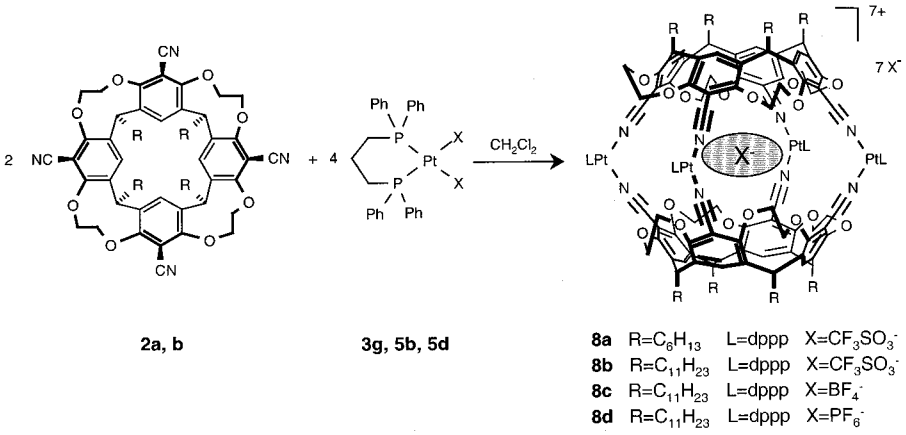

Table 3. Influence of Cavitand Preorganization on Cage Self-Assembly (CSA)

Entry	Organometallic precursor	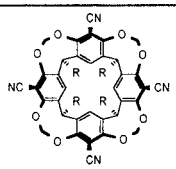 **1b** R=$C_{11}H_{23}$	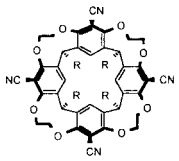 **2b** R=$C_{11}H_{23}$
1	Pd(dppm)$(OTf)_2$ **(3a)**	No CSA	No CSA
2	Pd(dppe)$(OTf)_2$ **(3c)**	No CSA	No CSA
3	Pd(dppp)$(OTf)_2$ **(3f)**	CSA **(7b)**	No CSA
4	Pd(dppp)$(BF_4)_2$ **(5a)**	CSA **(7h)**	No CSA
5	Pd(dppp)$(PF_6)_2$ **(5c)**	CSA **(7k)**	No CSA
6	Pd(dppb)$(OTf)_2$ **(3h)**	CSA **(7f)**[a]	No CSA
7	Pt(dppp)$(OTf)_2$ **(3g)**	CSA **(7d)**	CSA **(8b)**[b]
8	Pt(dppp)$(BF_4)_2$ **(5b)**	CSA **(7i)**	CSA **(8c)**[b]
9	Pt(dppp)$(PF_6)_2$ **(5d)**	CSA **(7j)**	CSA **(8d)**[b]

[a] The CSA is partial at 300 K and complete at 373 K. [b] The CSA is partial at 300 K and complete at 353 K.

rigidity of the tetradentate cavitand ligand and the relative orientation of the four cyano substituents on the cage self-assembly have been evaluated, introducing conformationally mobile ethylene-bridged cavitands **2a**,**b** (Scheme 3). In the C_{4v}-cone conformer the four nitriles of **2a**,**b** assume an even more diverging spatial orientation with respect to their methylene-bridged analogues, i.e., they form a wider α angle relative to the C_4 symmetry axis (see drawing I),[16] closer to the 45° angle ideal for the formation of strainless square-planar complexes. Computer modeling (Spartan 5.1, Wavefunction Inc.) of cages **7** and **8** suggested the formation of less strained square-planar complexes in the case of **8**. Table 3 reports the real outcome of the self-assembly process between cavitand **2b** and several organometallic precursors compared to the case of **1b**. In the case of **2b**, CSA is possible only with Pt complexes, which provide sufficient coordinative strength toward nitriles to freeze the cavitand in the required cone conformation. Their Pd analogues failed to give CSA under the same conditions. Also in this case inclusion of a single anion has been detected by ^{19}F NMR. A second interesting feature connected to the use of ethylene-bridged cavitands **2a**,**b** is the temperature effect on CSA: in all cases the process is partial at 300 K and complete only above 350 K (Figure 2). This unusual temperature effect led us to investigate the thermodynamics and kinetics of CSA. The different behavior of **2b** vs **1b** in the self-assembly process points out that, in terms of preorganization of the cavitand ligands, conformational rigidity is more important than optimal coordination geometry.

Finally, CSA does not require the formation of all four square-planar complexes to be effective. Cavitand **9**, having only three

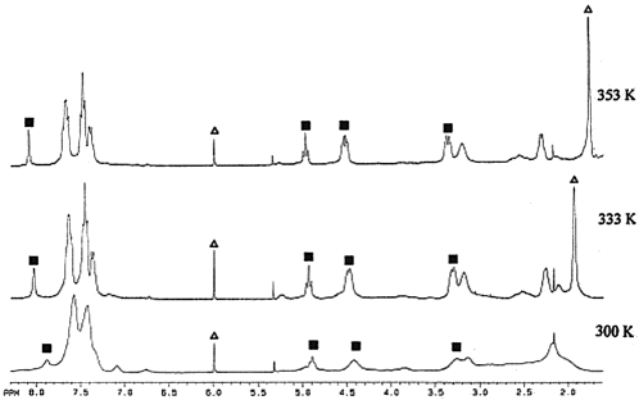

Figure 2. Equilibrium cage-oligomers for **8b** in $C_2D_2Cl_4$ monitored by ^{1}H NMR as a function of temperature (1:2 mixture of **2b** and **3g**): (■) diagnostic signals of the cage; (△) solvent and water resonances.

cyano substituents at the upper rim, in the presence of 3 equiv of Pt(dppp)$(OTf)_2$, led to the quantitative formation of capsule **10** (Scheme 4). Interestingly in this case no inclusion of a triflate counterion was detected by ^{19}F NMR. This experimental evidence can be interpreted in two ways: (a) the cavity no longer has a thermodynamic affinity for triflate; (b) the guest exchange in and out the cavity is fast on the NMR time scale, due to the presence of a wide portal in the equatorial region of the capsule, large enough to allow the escape of the triflate ion from the interior of the cage. In the second case a change in the chemical shift ($\Delta\delta$) of all triflates should be observed, as the average of two situations (bound and free triflate). The δ value of the bound triflate must be measured in order to evaluate the $\Delta\delta$. Since we have been unable to determine the chemical shift of the bound triflate in **10** from low-temperature spectra, we cannot distinguish between the two possibilities.

Thermodynamics and Kinetics of the CSA. The self-assembly process of methylene-bridged cages **7b** and **7d** has been monitored by ^{1}H NMR and FT-IR. In particular in the case of ^{1}H NMR experiments, the stepwise addition of metal precursors **3f**−**g** to cavitand **1b** led to the appearance of the diagnostic peaks of the cages and to the disappearance of those of the limiting reactant.[9a] Likewise for FT-IR the changes in nitrile absorption in the triple bond stretching region of the spectrum were monitored (see Supporting Information). In both cases the self-assembly process turned out to be highly cooperative: the coordination cage was the only product observed even in the presence of an excess of either one of the two reactants. No intermediates in the self-assembly process were observed. This is consistent with the rapid formation of the thermodynamically favored cage with respect to other species. Variable temperature ^{1}H NMR was performed on cage **7d** between 213 and 353 K. Only below 253 K did oligomeric

Scheme 4

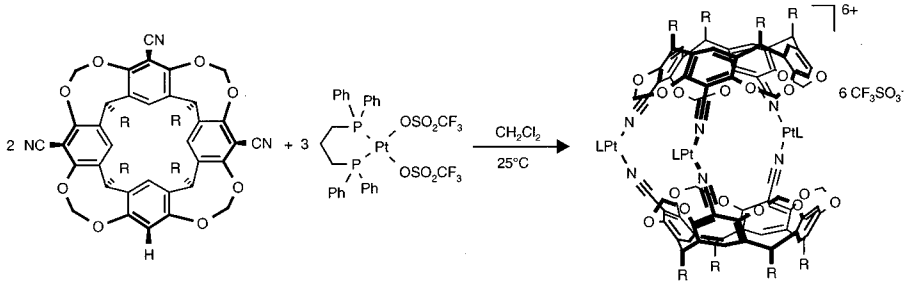

9 R=$C_{11}H_{23}$ **10** R=$C_{11}H_{23}$ L=dppp

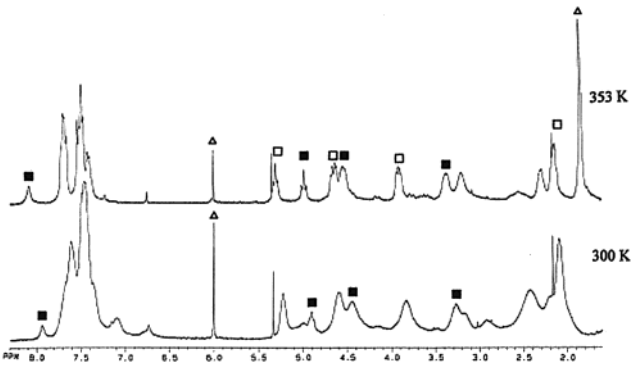

Figure 3. Equilibrium cage-oligomers for **8b** in $C_2D_2Cl_4$ monitored by ^{1}H NMR as a function of temperature using a 1:1 stoichiometric ratio of **2b** and **3g**: (■) diagnostic signals of the cage; (□) signals of uncomplexed cavitand **2b**; (△) solvent and water resonances.

species started to compete with **7d**, as indicated by broadening of the spectrum and the appearance of new peaks.

This picture changed dramatically when cavitand **2b** was used in the self-assembly process: the ^{1}H NMR spectra recorded by mixing **2b** and Pt(dppp)(OTf)$_2$ **3g** in a 1:1 stoichiometric ratio at 300 K exhibited broad signals, as well as signals belonging to cage **8b** (Figure 3). Upon heating to 353 K the spectrum became sharp, showing the presence of **8b** plus unreacted cavitand **2b**. Higher temperatures did not lead to further changes. When the temperature was lowered again to 300 K, the spectrum returned to the original pattern; this conveys a reversible process. In the case of a 1:2 stoichiometric ratio, the formation of oligomers is still favored at 300 K, in accordance with ES-MS data, while at 353 K the equilibrium is shifted toward the formation of **8b** (Figure 2). The same behavior was observed using chelating ligands forming P−M−P angles which deviates from the optimal 90° value (see entries 4 and 9 of Table 1).

Calorimetric experiments were conducted in tetrachloroethane as solvent at different temperatures to quantify the enthalpic contribution to the self-assembly. Both processes are strongly endothermic: $\Delta H^{\varnothing} = +57.7 \pm 0.7$ kJ mol^{-1} for cage **7d** formation at 298 K and $\Delta H^{\varnothing} = +60 \pm 2$ kJ mol^{-1} for cage **8b** formation at 343 K,[17] the temperature at which **8b** is almost completely assembled. The formation of both cages is therefore *entropy driven*, with the temperature range of the equilibrium cage-oligomers governed by the level of preorganization of the cavitand components.[18]

ES-MS experiments were performed in acetone at room temperature to confirm the existence in solution of other adducts of **2b** plus Pt(dppp)(OTf)$_2$ besides cage **8b**. In the case of **7d** the dominant species in acetone detected as $[M - 2CF_3SO_3^-]^{2+}$ was *m*/*z* 2916.0, identified as [cage **7d**]$^{2+}$ (Figure 4a). By contrast, in the case of **8b**, the primary species was observed at *m*/*z* 2066.3 and corresponds to [**2b**$_2$·(Pt-complex)$_2$]$^{2+}$ either in the form of partially formed cage or open dimer. The other two major species detected were respectively *m*/*z* 2971.8, identified

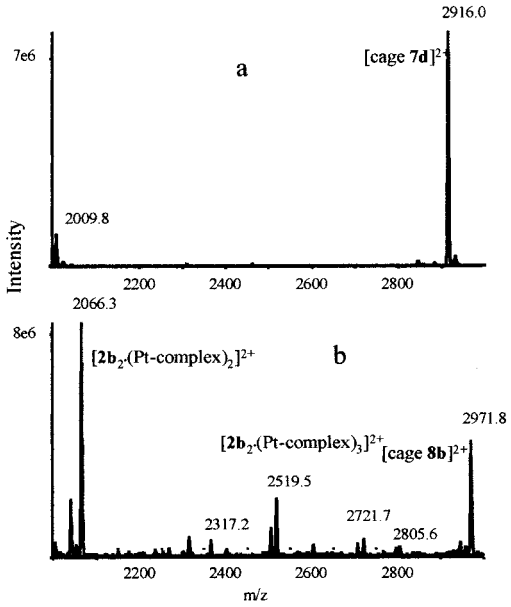

Figure 4. ES-MS spectra at 298 K of acetone solutions of (a) cage **7d** (100 μM) and (b) cage **8b** (100 μM) recorded under the same operating conditions.

as [cage **8b**]$^{2+}$, and *m*/*z* 2519.5, corresponding to [**2b**$_2$·(Pt-complex)$_3$]$^{2+}$ complex (Figure 4b).

The unusual temperature dependence of the CSA was further substantiated by dynamic ^{19}F NMR studies performed on cages **7d** and **8b**. Since the encapsulation of a triflate anion is diagnostic of cage formation, monitoring the resonance of the included triflate anion as a function of temperature is a simple and clean way to trace CSA. The overall size and the dimensions of the equatorial portals of the cavity are similar in methylene- and ethylene-bridged cages; therefore their encapsulation properties are comparable. Anion encapsulation follows the same temperature dependence observed by ^{1}H NMR. For cage **7d** triflate encapsulation is temperature independent from 253 K upward (Figure 5a), while for cage **8b** it increases with temperature from 253 K, where it is negligible, to 353 K, where it is complete (Figure 5b). The two cages manifest the same type of temperature dependence, only **7d** requires lower temperature to disassemble. This implies that CSA of **7d** is more strongly entropically driven than that for cage **8b**.

This unusual temperature dependence of self-assembly processes has been observed in hydrogen-bonded capsules hosting neutral guests[19] and in supramolecular clusters encapsulating cations.[20] In both examples, the origin of this unusual behavior has been attributed to the large entropic gain associated with the release of solvent upon encapsulation. Also in our case the endothermic nature of CSA can be rationalized in terms of desolvation of the cage components and particularly of the included anion[21] in the self-assembly process, which leads to the entropic overriding of the unfavorable positive $\Delta H^{\varnothing}$ of formation. Less evident is the reason for the enthalpic opposition when the encapsulation leads to a partial, electrostatic favorable, charge neutralization (the host charge is reduced from 8^+ to 7^+). A convincing explanation has been given by Raymond and

(16) In ref 10 several crystal structures of cavitands are reported, from which is possible to estimate the average C_4-aromatic ring α angle of 29° for methylene-bridged cavitands and 41° for ethylene-bridged cavitands. A close average C_4-aromatic ring α angle of 31° [range 30.1(3)° < α < 31.4(3)°] has been derived for methylene-bridged cavitand **1b** from the crystal structure of **7d**.

(17) Cage **8b** at 298 K is in equilibrium with many oligomeric species; therefore it is not possible to separate the various contributions to the overall heat of reaction.

(18) For the thermodynamics of self-assembly, see: (a) Chi, X.; Guerin, A. J.; Haycock, R. A.; Hunter, C. A.; Sarson, L. D. *J. Chem. Soc., Chem. Commun.* **1995**, 2563−2565. (b) Ercolani, G. *J. Phys. Chem. B* **1998**, *102*, 5699−5703.

(19) (a) Kang, J.; Rebek, J., Jr. *Nature* **1996**, *382*, 239−241. (b) Meissner, R.; Garcias, X.; Mecozzi, S.; Rebek, J., Jr. *J. Am. Chem. Soc.* **1997**, *119*, 77−85.

(20) (a) Parac, T. N.; Caulder, D. L.; Raymond, K. N. *J. Am. Chem. Soc.* **1998**, *120*, 8003−8004. (b) Parac, T. N.; Scherer, M.; Raymond, K. N. *Angew. Chem., Int. Ed.* **2000**, *39*, 1239−1242.

(21) For an example of entropy-driven anion complexation, see: Berger, M.; Schmidtchen, F. P. *Angew. Chem., Int. Ed.* **1998**, *37*, 2694−2696.

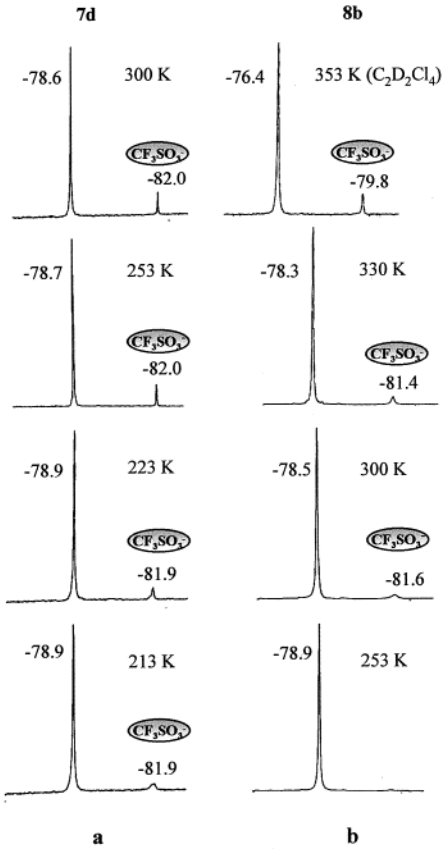

Figure 5. Variable temperature 188 MHz ^{19}F NMR spectra of (a) cage **7d** and (b) cage **8b** in $CDCl_3$.

co-workers[20a] by taking into account the large enthalpic costs associated with ion desolvation. According to this interpretation, anions with small solvation enthalpies should be preferentially encapsulated, provided that they fit into the cavity. To verify this hypothesis, we undertook a series of anion exchange experiments to test the selectivity in anion encapsulation. The results are reported in a following paragraph.

Since the anion exchange experiments require dissociation/recombination of the coordination cages, the kinetic stability of Pd and Pt cages deserves special attention. A rough estimate of the dissociation/recombination time scale can be obtained by monitoring via ^{1}H NMR the ligand exchange between a preformed cage and a competitive ligand. This estimate, albeit not accurate, is sufficient for the purpose of choosing the optimal anion exchange conditions.[22] Two set of experiments were performed directly in the NMR tube. Addition of cavitand **1c** to a $CDCl_3$ solution of cage **7b** at 300 K led to the immediate formation of three new species in solution, identified respectively as cavitand **1b**, Pd heterocage **11**, and Pd homocage **12**, and to the decrease of **7b** (Scheme 5). The five species were identified through the diagnostic signals of the methylene bridge CH_{in} and resorcinarene CH and ArH protons, and their presence in solution was confirmed by ES-MS. Further addition of **1c** led to an increase in the concentration of **1b**, **11**, and **12** with concomitant decrease of **7b**. In the same experiment performed on Pt cage **7d**, the ligand exchange is negligible immediately after the addition, with an equilibration time of over 4 h at 300 K. The same experiment, repeated at 330 K, led to immediate ligand exchange. Therefore, the dynamics of dissociation/recombination, slow on the NMR time scale in both cages, is fast on the human time scale at ambient temperature only for **7b**, a further evidence of the greater strength of the Pt−NC dative bond compared to the Pd−NC one.

Self-Selection of the Cavitand Subunits. The relative stability of cages **7d** and **8b** has been assessed and exploited in competition experiments. The selective formation of cage **7d** was proven by adding 2 equiv of $Pt(dppp)(OTf)_2$ **3g** to a solution of a 1:1 molar ratio of cavitands **1b** and **2b** in $CDCl_3$. The self-assembly process, monitored by ^{1}H NMR, gave cage **7d** as the only product, while the flexible ethylene-bridged cavitand **2b** remained unchanged in solution. The same reaction performed in the presence of an excess of $Pt(dppp)(OTf)_2$ at 330 K led to the exclusive formation of both homocages **7d** and **8b**, with no trace of the heterocage having both cavitands as components (Scheme 6). Selective disassembly of Pt cages was also realized: reaction of equimolar amounts of cages **7d** and **8b** in $CDCl_3$ with the competitive ligand NEt_3, in sufficient quantity to disassemble only one cage, left **7d** unchanged, while **8b** was completely disassembled. This was clearly visible from the ^{1}H NMR spectrum which showed the characteristic signal patterns of **2b** and **7d**. The small mismatch between the biting angles of the nitriles of the two cavitand ligands is sufficient to suppress heterocage formation. This is a further evidence of how sensitive CSA is to the preorganization of the molecular components, both in terms of process activation and product selectivity.

Selectivity in Anion Encapsulation. The Born equation[23] allows for estimation of the free energy of solvation of an ion of radius r (Å)[24] and charge z in a given solvent. For monovalent anions such as BF_4^-, PF_6^-, and $CF_3SO_3^-$ in chloroform, we have $\Delta G^\circ_{m,solv} = -550r^{-1}$ kJ mol^{-1}. Since encapsulation requires desolvation of the anion, our expectation was that inclusion selectivity in a given cage would have been dictated by the relative entalphy of solvation of the anions, thus favoring the larger, less solvated ones. Accordingly, in our case the predicted selectivity should have been $CF_3SO_3^- > PF_6^- > BF_4^-$. Table 4 reports the observed selectivity in anion encapsulation by methylene-bridged cages for competition experiments such as the one depicted in Scheme 7, monitored at two different temperatures by ^{1}H and ^{19}F NMR. Two trends are observed: (i) at 300 K in the presence of stoichiometric amounts of the competing ion, the encapsulation preference is in the order $BF_4^- > CF_3SO_3^- \gg PF_6^-$, which becomes complete for BF_4^- in the presence of an excess of $(NBu_4^+)(BF_4^-)$; (ii) at 333 K under stoichiometric conditions the slight prevalence of BF_4^- vs $CF_3SO_3^-$ is reversed in favor of the latter.

The discrepancy between observed and expected selectivity in anion encapsulation led us to further investigate the matter both experimentally and via computer modeling. ES-MS turned out to be, once again, a very valuable investigation tool, enabling us to detect the presence of solvent molecules trapped within the cages.[25] For all cages having $CF_3SO_3^-$ and PF_6^- as counterions, ES-MS gave $[M - 2X]^{2+}$ and $[M - 3X]^{3+}$ as prominent ions, both in chloroform and acetone as solvents, while in the case of BF_4^- the base peaks correspond to the m/z values expected for $[CHCl_3@M - 2BF_4]^{2+}$, $[CHCl_3@M - 3BF_4]^{3+}$, $[acetone@M - 2BF_4]^{2+}$, and $[acetone@M - 3BF_4]^{3+}$ respectively (see Figure 6 in the case of chloroform). These results imply that only in the case of encapsulated BF_4^- is there

(22) For a detailed NMR study of the exchange process in hydrogen-bonded cali[4]arenes capsules, see: Mogck, O.; Pons, M.; Böhmer, V.; Vogt, W. *J. Am. Chem. Soc.* **1997**, *119*, 5706−5712.

(23) (a) Moore, W. J. In *Physical Chemistry*, 5th ed.; Longman Group Limited: London, 1976; p 430. (b) Marcus, Y. In *Ion Solvation*; Wiley & Sons: Chichester, 1985.

(24) Even if the Born equation is strictly valid only for spherical ions, it gives a good approximation of $\Delta G^\circ_{m,solv}$ also for nonspherical ones.

(25) Schalley, C. A.; Castellano, R. K.; Brody, M. S.; Rudkevich, D. M.; Siuzdak, G.; Rebek, J., Jr. *J. Am. Chem. Soc.* **1999**, *121*, 4568−4579.

Scheme 5

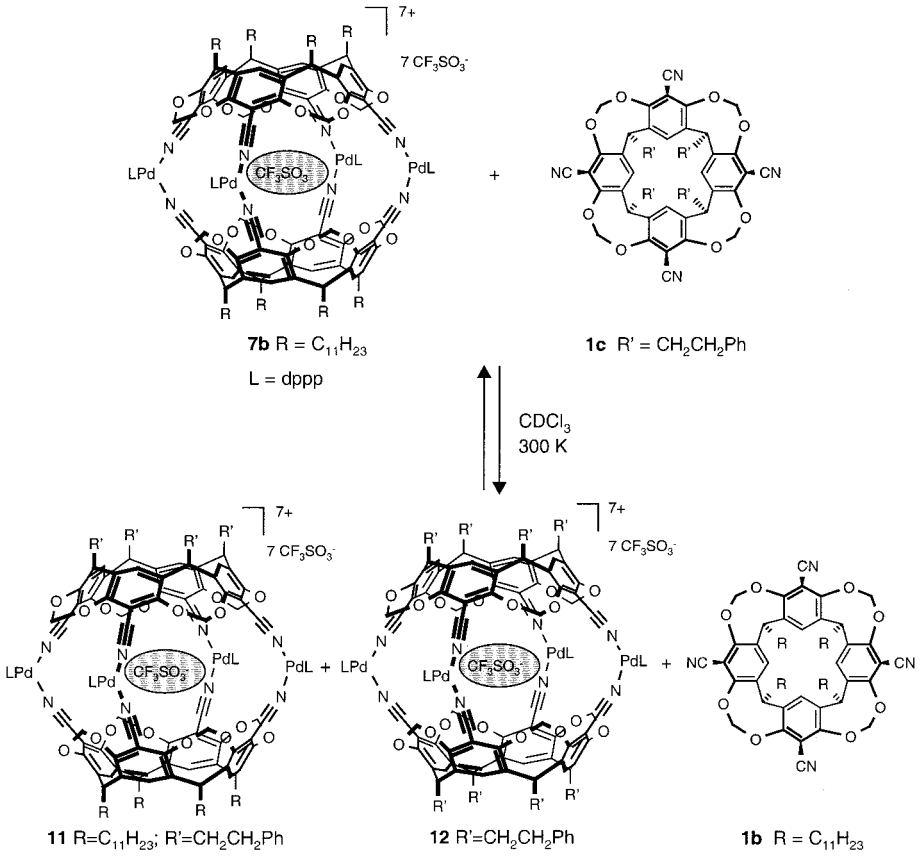

Scheme 6

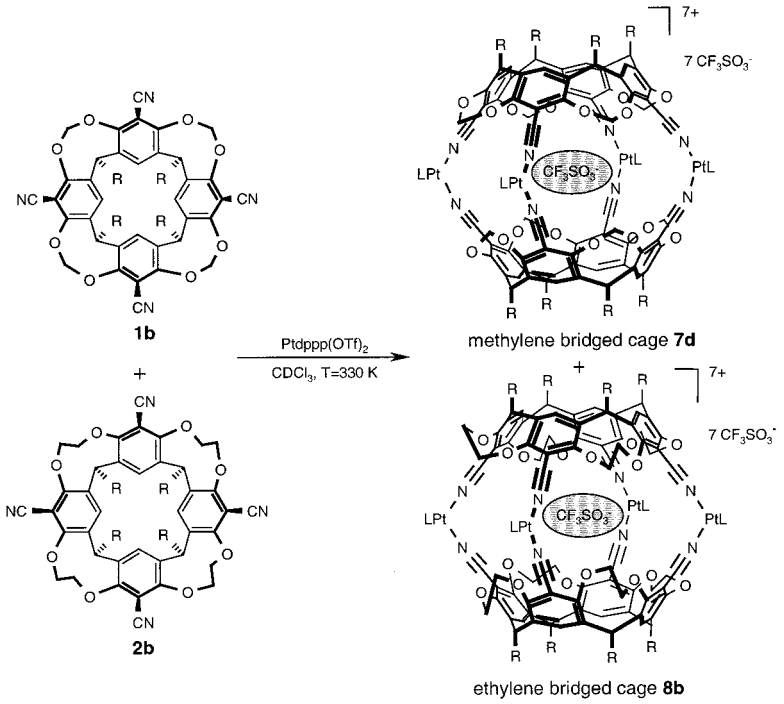

room enough in the cavity for one molecule of solvent, while in the other two cases the anion is included alone, as proven for the case of $CF_3SO_3^-$ by the crystal structure.

Molecular modeling was carried out to confirm the experimental findings using the GRASP program.[26] From the crystal structure of **7d** the volume of the internal cavity has been estimated in 248 Å^3 with a spherical probe of diameter 1.7 Å.[27] The van der Waals molecular volumes of BF_4^-, PF_6^-, $CF_3SO_3^-$, acetone, and chloroform were also calculated with GRASP using the same probe. If a single guest is encapsulated, the resulting occupancy factor[28] is small, well below the reported optimal value of 0.55 (Table 5).[26b] When two species (anion + solvent)[29]

(26) (a) Nicholls, A.; Sharp, K.; Honig, B. *Proteins* **1991**, *11*, 281−296. (b) Mecozzi, S.; Rebek, J., Jr. *Chem. Eur. J.* **1998**, *6*, 1016−1022.

Table 4. Guest Inclusion Ratio Based on ^{1}H NMR and ^{19}F NMR

cage	*T* (K)	$(NBu_4^+)(BF_4^-)$ stoichiometric (8 equiv)	$(NBu_4^+)(PF_6^-)$ stoichiometric (8 equiv)	$(NBu_4^+)(BF_4^-)$ excess (40 equiv)	$(NBu_4^+)(PF_6^-)$ excess (40 equiv)
Pt cage **7d**	300	$CDCl_3{\cdot}BF_4^- > CF_3SO_3^-$ $BF_4^-/CF_3SO_3^- = 1.3/1.0$	$CF_3SO_3^- \gg PF_6^-$	only $CDCl_3{\cdot}BF_4^-$	$CF_3SO_3^- > PF_6^-$
Pt cage **7d**	333	$CF_3SO_3^- > CDCl_3{\cdot}BF_4^-$ $CF_3SO_3^-/BF_4^- = 1.2/1.0$	$CF_3SO_3^- \gg PF_6^-$	$CDCl_3{\cdot}BF_4^- \gg CF_3SO_3^-$	$CF_3SO_3^- > PF_6^-$ $CF_3SO_3^-/PF_6^- = 1.3/1.0$
Pd cage **7b**	300	$CDCl_3{\cdot}BF_4^- > CF_3SO_3^-$ BF4-/$CF_3SO_3^- = 2.7/1.0$	only $CF_3SO_3^-$	only $CDCl_3{\cdot}BF_4^-$	only $CF_3SO_3^-$
Pd cage **7b**	333	$CF_3SO_3^- > CDCl_3{\cdot}BF_4^-$ $CF_3SO_3^-/BF_4^- = 1.2/1.0$	only $CF_3SO_3^-$	$CDCl_3{\cdot}BF_4^- \gg CF_3SO_3^-$	only $CF_3SO_3^-$

Scheme 7

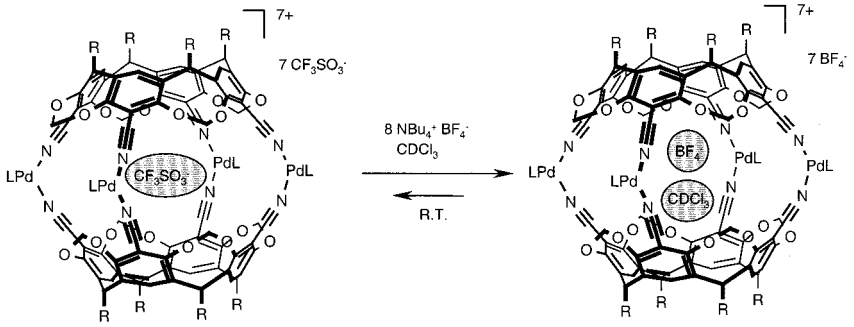

are encapsulated together, the geometrical constraints imposed by the shapes of the guests must also be considered to evaluate the possible occupancy of the cage. The problem has been approached using the docking functions of Spartan (version 5.1, Wavefuction Inc.) and Sybyl (version 6.5, Tripos Inc.) softwares, implemented with the GRASP van der Waals molecular volumes of the guests. Both programs led to the same results for the energy-minimized structures of $BF_4^-{\cdot}CHCl_3$@cage, $PF_6^-{\cdot}CHCl_3$@cage, and $CF_3SO_3^-{\cdot}CHCl_3$@cage (Figure 7 in which part of the cavity walls have been cut away for easy of visualization). The pictures clearly show that for the larger triflate and hexafluorophosphate anions there is overlap among the van der Waals spheres of the two guests, absent in the case of tetrafluoborate anion. The resulting steric hindrance prevents the inclusion of the solvent molecule for $CF_3SO_3^-$ and PF_6^-.

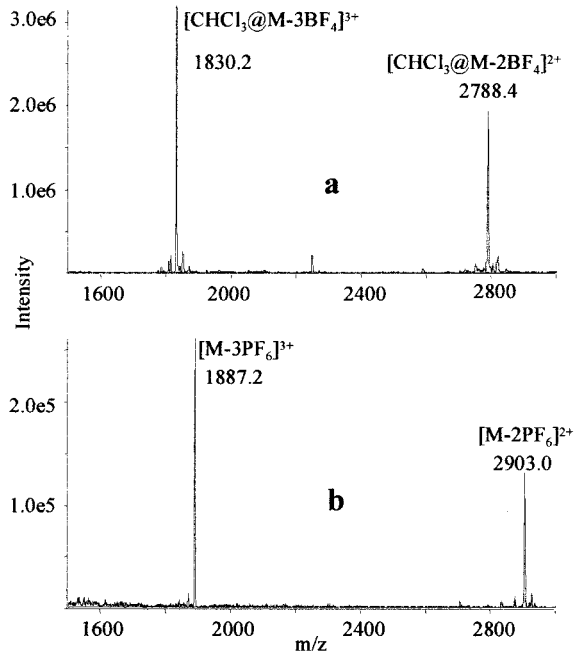

Figure 6. ES-MS spectra of $CHCl_3$ solutions of (a) cage **7i** (50 μM) and (b) cage **7j** (50 μM).

Table 5. Molecular Volumes and Occupancy Factors for Anionic and Neutral Guests in Cage **7d**

guest	vol (Å^3)	occupancy factor
BF_4^-	37	0.15
PF_6^-	66	0.27
$CF_3SO_3^-$	86	0.35
acetone	61	0.25
chloroform	68	0.27

ES-MS and molecular modeling together provide a consistent molecular description of the observed encapsulation properties of cavitand-based coordination cages. Only for BF_4^- is the cavity sufficiently wide to accommodate an ancillary solvent molecule, thus reducing the enthalpic cost required for the desolvation of BF_4^-. This renders BF_4^- the preferred encapsulated anion at 300 K. The change in selectivity observed upon increasing the temperature to 333 K is the result of the higher cage occupancy factor of $BF_4^-{\cdot}CHCl_3$ with respect to $CF_3SO_3^-$. At higher temperatures the entropic term favors $CF_3SO_3^-$, since its movements are less restricted in the confined space of the cavity with respect to the couple $BF_4^-{\cdot}CHCl_3$. This additional entropic cost for $BF_4^-{\cdot}CHCl_3$ is sufficient to reverse to selectivity pattern observed at 300 K, as theoretically predicted by Mecozzi and Rebek for neutral guest encapsulation.[26b] To the best of our knowledge, this is the first time that such an effect has been experimentally observed.

Conclusions

In this paper we have presented a complete characterization of cavitand-based coordination cages and a comprehensive study of the factors affecting the self-assembly process. The following

(27) The 1.7 Å probe is the smallest one which does not fall out of the lateral portals of the cage.

(28) The occupancy factor of a guest molecule in the cavity of a host is defined as the ratio of the van der Waals molecular volume of the guest to the volume of the cavity calculated on the van der Waals interior surface of the host (ref 19b).

(29) The possibility of encapsulating two anions in one cage has been excluded due to electrostatic repulsion.

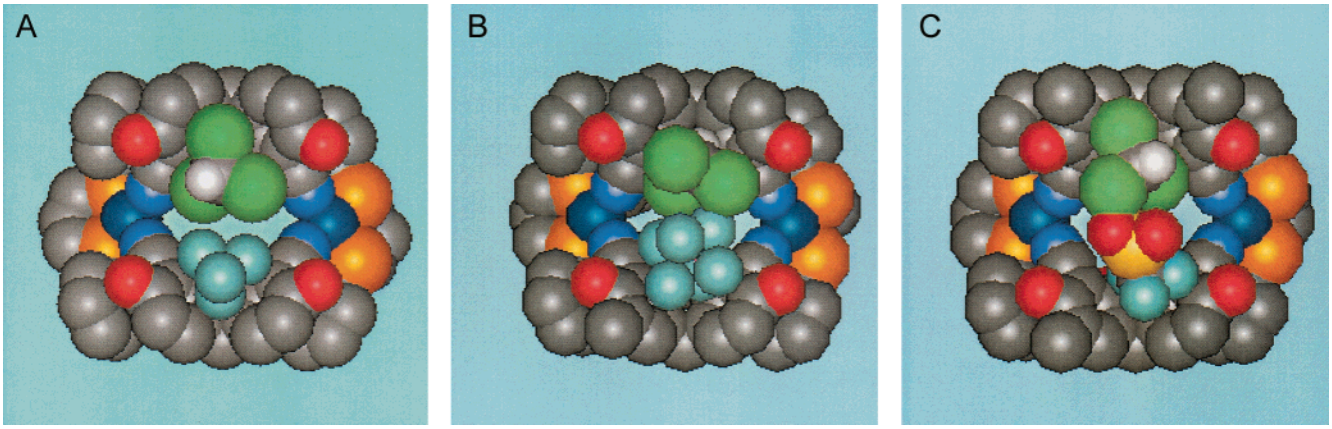

Figure 7. CPK representation of the vertical cross-section of cage **7d** with encapsulated (A) $CHCl_3 \cdot BF_4^-$; (B) $CHCl_3 \cdot PF_6^-$; (C) $CHCl_3 \cdot CF_3SO_3^-$.

structural parameters have been found to be the key factors controlling CSA: (i) a P−M−P angle close to 90° between the chelating ligand and the metal precursor; (ii) Pd and Pt as metal centers; (iii) a weakly coordinated counterion; (iv) preorganization of the tetradentate cavitand ligand. CSA is extremely sensitive to structural variations in the metal precursor: small deviations from the optimal parameters completely switch off the process. On the other hand, the level of preorganization of the cavitand ligand influences the equilibrium cage-oligomers, favoring cage formation. The ethylene-bridged cages **8** are thermodynamically less stable than the methylene-bridged ones **7**, due to the residual conformational mobility of **2**, which requires an entropic price to be paid for freezing **2** in the cone conformation necessary for CSA. In addition, a mismatch between the biting angles of the nitriles of the two cavitand ligands is not tolerated by CSA, suppressing heterocage formation.

Dynamic ^1H and ^{19}F NMR experiments and calorimetric measurements clearly indicate that CSA is entropy driven, with the enthalpic cost of desolvating the molecular components, and particularly the encapsulated anion, compensated by the large entropic gain associated with the release of the solvent molecules into the bulk. Desolvation is pivotal also in determining selectivity in anion encapsulation, together with cavity size. Dimensions and shape of the cavity perturb the basic selectivity pattern, dictated by the relative solvation enthalpy of the guests, by allowing the entrance of a solvent molecule only in the case of BF_4^-, thus favoring it with respect to the other ions.

The potential of this self-assembly process in terms of quantitative, selective, and reversible formation of molecular cages can be fully exploited when all the critical factors determining the outcome of the process are understood and rationalized. In this respect, the self-assembly protocol emerging from this study has been employed in the surface-controlled generation of coordination cages, using self-assembled monolayers (SAMs) as molecular components.[30]

Experimental Section

General Methods. All reactions were conducted under an argon atmosphere. FT-IR spectra were recorded on a Nicolet 5PC spectrometer. NMR spectra were recorded on Bruker XP200, AC300, and AMX400 spectrometers. ^1H NMR were recorded at 300 and 400 MHz, and all chemical shifts (δ) were reported in ppm relative to the proton resonance resulting from incomplete deuteration of the NMR solvent: $CDCl_3$ (7.24 ppm), CD_2Cl_2 (5.32 ppm), $C_2D_2Cl_4$ (6.0 ppm). ^{13}C NMR spectra were recorded at 75 MHz, and all chemical shifts were reported in ppm relative to the carbon resonance of the deuterated NMR solvent: $CDCl_3$ (77.0 ppm). ^{31}P NMR spectra were recorded at 81 and 161 MHz, and all chemical shifts were reported in ppm relative to external 85% H_3PO_4 at 0.00 ppm. ^{19}F NMR spectra were recorded at 188 MHz, and all chemical shifts were reported relative to external $CFCl_3$ at 0.00 ppm. Melting points were obtained with a Electrothermal capillary melting points apparatus and were not corrected. Mass spectra of the organic compounds were measured with a Finningan-MAT SSQ 710 spectrometer using the CI (chemical ionization) technique. Microanalyses were performed by the service of Parma University. Thin-layer chromatography (TLC) was performed on commercially prepared silica gel $60F_{254}$ plates purchased by Merck, and column chromatography was performed using Merck 230−400 mesh silica gel 60. Flash column chromatography was performed with silica gel 60 (Merck 230−400 mesh).

Materials. All commercial reagents were ACS reagent grade and used as received. Diethyl ether and THF were dried and distilled over Na/benzophenone. All the other solvents were dried over 3 and 4 Å molecular sieves. All solvents were freeze−thaw−pump degassed three times before use. All octols,[31] tetrabromo octols, and tetrabromo methylene/ethylene-bridged cavitands[10,32] were prepared following modified literature procedures (Supporting Information). Complexes **3a**−**h** and **4a** were prepared from the corresponding dichlorobis derivatives following a established procedures.[33]

General Procedure for the Synthesis of Tetracyanocavitands. To a stirred solution of tetrabromo cavitand (2 mmol) in 1-methyl-2-pyrrolidinone was added CuCN (1.39 g, 15.5 mmol). The reaction mixture was heated at reflux (210 °C) for 12 h and then cooled to 80 °C. A mixture composed of water (85 mL), hydrochloric acid (29 mL), and $FeCl_3$ (5.11 g, 31.5 mmol) was poured in it, and the solution was stirred for 1 h. After cooling to room temperature, the resulting brown precipitate was filtered and washed with water.

7,11,15,28-Tetracyano-1,21,23,25-tetrahexyl-2,20:3,19-dimetheno-1*H*,21*H*,23*H*,25*H*-bis[1,3]dioxocino[5,4-*i*:5′,4′-*i*′]benzo[1,2-*d*:5,4-*d*′]-bis[1,3]benzodioxocino (1a). Purification of the crude by chromatography on silica gel (eluant CH_2Cl_2/hexane/acetone 95:2:3, $R_f = 0.6$) gave cavitand **1a** as a white solid (70% yield): mp >300 °C; ^1H NMR ($CDCl_3$, 300 MHz) δ 0.89 (t, 12H, CH_3), 1.25−1.43 [m, 32H, CH_2-(CH_2)$_4$ CH_3], 2.19 [m, 8H, CHCH_2(CH_2)$_4$$CH_3$], 4.57 (d, 4H, OC$H_{in}$O, $J = 6.7$ Hz), 4.80 [t, 4H, CHCH_2(CH_2)$_4$$CH_3$], 6.08 (d, 4H, OC$H_{out}$O, $J = 6.7$ Hz), 7.26 (s, 4H, ArH); ^{13}C NMR ($CDCl_3$, 75 MHz) δ 13.9 (CH_3), 22.5, 27.5, 29.2, 31.7 (CH_2), 36.2 (*C*H), 98.8 (OCH_2O), 104.4 (*C*N), 111.9 (C_{ipso}), 124.6 (C_p), 139.0 (C_m), 156.2 (C_o); IR (KBr) 2233

(30) Levi, S.; Guatteri, P.; van Veggel, F. C. J. M.; Vancso, J.; Dalcanale, E.; Reinhoudt, D. N. *Angew. Chem., Int. Ed.* **2001**, *40*, 1892−1896.

(31) Tunstad, L. M.; Tucker, J. A.; Dalcanale, E.; Weiser, J.; Bryant, J. A.; Sherman, J. C.; Helgeson, R. C.; Knobler, C. B.; Cram, D. J. *J. Org. Chem.* **1989**, *54*, 1305−1312.

(32) Román, E.; Peinador, C.; Mendoza, S.; Kaifer, A. E. *J. Org. Chem.* **1999**, *64*, 2577−2578.

(33) (a) Fallis, S.; Anderson, G. K.; Rath, N. P. *Organometallics* **1991**, *10*, 3180−3184. (b) Stang, P. J.; Cao, D. H.; Saito, S.; Arif, A. M. *J. Am. Chem. Soc.* **1995**, *117*, 6273−6283.

cm^{-1} (C≡N); MS (CI) *m*/*z* 973 (M$^+$, 100). Anal. Calcd for $C_{60}H_{68}N_4O_8$: C, 74.05; H, 7.04; N 5.76. Found: C, 73.92; H, 7.23; N, 5.68.

7,11,15,28-Tetracyano-1,21,23,25-tetraundecyl-2,20:3,19-dimetheno-1*H*,21*H*,23*H*,25*H*-bis[1,3]dioxocino[5,4-*i*:5′,4′-*i*′]benzo[1,2-*d*:5,4-*d*′]-bis[1,3]benzodioxocin (1b). Silica gel column chromatography of the crude (eluant 90:9:1 methylene chloride:hexane:acetone) gave compound **1b** as the major product (TLC R_f = 0.6, 70% yield) and the tricyano derivative **9** as a byproduct (TLC R_f = 0.4, 14% yield).

1b: mp 216−218 °C; ^{1}H NMR (300 MHz, $CDCl_3$) δ 0.88 (t, 12H, C*H*$_3$), 1.26−1.40 [m, 72H, CH$_2$(C*H*$_2$)$_9$CH$_3$], 2.19 [m, 8H, CHC*H*$_2$(CH$_2$)$_9$CH$_3$], 4.59 (d, 4H, OC*H*$_{in}$O, J = 6.7 Hz), 4.79 [t, 4H, C*H*CH$_2$(CH$_2$)$_9$CH$_3$], 6.08 (d, 4H, OC*H*$_{out}$O, J = 6.7 Hz), 7.25 (s, 4H, Ar*H*); ^{13}C NMR (75 MHz, $CDCl_3$) δ 14.1 (*C*H$_3$), 22.7, 27.6, 29.2, 29.4, 29.5, 29.6, 31.9 (*C*H$_2$)$_{10}$, 36.2 (*C*H), 98.8 (O*C*H$_2$O), 104.4 (*C*N), 111.9 (*C*$_{ipso}$), 124.7 (*C*$_p$), 139.1 (*C*$_m$), 156.2 (*C*$_o$); IR (KBr) 2238 cm^{-1} (C≡N); MS (CI) *m*/*z* 1254 (M$^+$, 100). Anal. Calcd for $C_{80}H_{108}N_4O_8$: C, 76.64; H, 8.68; N 4.47. Found: C, 76.49; H, 8.81; N, 4.38.

9: mp 140−143 °C; ^{1}H NMR (300 MHz, $CDCl_3$) δ 0.87 (t, 12H, C*H*$_3$), 1.34 [m, 72H, CHCH$_2$(C*H*$_2$)$_9$CH$_3$], 2.19 [m, 8H, CHC*H*$_2$(CH$_2$)$_9$CH$_3$], 4.47 (d, 2H, OC*H*$_{in}$O, J = 7.3 Hz), 4.60 (d, 2H, OC*H*$_{in}$O, J = 7.4 Hz), 4.76 (m, 4H, C*H*C$_{11}$H$_{23}$), 5.91 (d, 2H, OC*H*$_{out}$O, J = 7.3 Hz), 6.06 (d, 2H, OC*H*$_{out}$O, J = 7.4 Hz), 6.59 (s, 1H, Ar*H*), 7.05 (s, 1H, Ar*H*), 7.29 (s, 3H, Ar*H*); ^{13}C NMR (75 MHz, $CDCl_3$) δ 14.0 (*C*H$_3$), 22.6−31.9 (*C*H$_2$)$_{10}$, 36.2 (*C*H), 98.8 (O*C*H$_2$O), 99.3 (O*C*H$_2$O), 104.0, 104.1 (*C*N), 112.4 (*C*$_{ipso}$), 117.0 (*C*H$_b$), 120.3, 124.9 (*C*$_p$), 138.1, 138.3, 139.1, 140.0 (*C*$_m$), 155.0, 155.7, 156.2, 156.7 (*C*$_o$); IR (KBr) 2233 cm^{-1} (C≡N); MS (CI) *m*/*z* 1229 (M$^+$, 100).

7,11,15,28-Tetracyano-1,21,23,25-tetrakis(2-phenethyl)-2,20:3,19-dimetheno-1*H*,21*H*,23*H*,25*H*-bis[1,3]dioxocino[5,4-*i*:5′,4′-*i*′]benzo-[1,2-*d*:5,4-*d*′]bis[1,3]benzodioxocin (1c). The collected solid was purified by silica gel flash chromatography, eluting with a mixture of methylene chloride:hexane:acetone 90:9:1, TLC R_f = 0.3. Compound **1c** was obtained as a white solid (61% yield): mp >300 °C; ^{1}H NMR (300 MHz, $CDCl_3$) δ 2.52 (m, 8H, CHC*H*$_2$CH$_2$C$_6$H$_5$), 2.66 (m, 8H, CHCH$_2$C*H*$_2$C$_6$H$_5$), 4.61 (d, 4H, OC*H*$_{in}$O, J = 7.5 Hz), 4.91 (t, 4H, C*H*CH$_2$CH$_2$), 6.11 (d, 4H, OC*H*$_{out}$O, J = 7.5 Hz), 7.09−7.38 (m, 24H, C$_6$*H*$_5$ + Ar*H*); IR (KBr) 2235 cm^{-1} (C≡N); MS (CI) *m*/*z* 1053 (MH$^+$, 100). Anal. Calcd for $C_{68}H_{52}N_4O_8$: C, 77.55; H, 4.98; N 5.32. Found: C, 77.50; H, 4.88; N, 5.48.

8,13,18,32-Tetracyano-5,6,10,11,15,16,20,21-octahydro-1,25,27,-29-tetrahexyl-2,24:3,23-dimetheno-1*H*,25*H*,27*H*,29*H*-bis[1,4]dioxonino-[6,5-*j*:6′,5′-*j*′]benzo[1,2-*e*:5,4-*e*′]bis[1,4]benzodioxonin (2a). Silica gel column chromatography of the crude (eluant 97.5:2.5 methylene chloride:acetone) gave compound **2a** as a white solid (67% yield): mp >300 °C;^{1}H NMR ($CDCl_3$, 300 MHz) δ 0.87 [t, 12H, CHCH$_2$-(CH$_2$)$_4$C*H*$_3$], 1.19−1.35 [m, 32H, CHCH$_2$(C*H*$_2$)$_4$CH$_3$], 2.07 [m, 8H, CHC*H*$_2$(CH$_2$)$_4$CH$_3$], 3.80 (m, 8H, OC*H*$_{in}$C*H*$_{in}$O), 4.58 (m, 8H, OC*H*$_{out}$C*H*-$_{out}$O), 5.22 (t, 4H, C*H*C$_6$H$_{13}$), 7.41 (s, 4H, Ar*H*); ^{1}H NMR (acetone-d_6, 300 MHz) δ 0.86 [t, 12H, CHCH$_2$(CH$_2$)$_4$C*H*$_3$], 1.22−1.35 [m, 32H, CHCH$_2$(C*H*$_2$)$_4$CH$_3$], 2.27 [m, 8H, CHC*H*$_2$(CH$_2$)$_4$CH$_3$], 3.89 (m, 8H, OC*H*$_{in}$C*H*$_{in}$O), 4.56 (m, 8H, OC*H*$_{out}$C*H*$_{out}$O), 5.30 (t, 4H, C*H*C$_6$H$_{13}$), 8.12 (s, 4H, Ar*H*); ^{13}C NMR ($CDCl_3$, 75 MHz) δ 13.9 (*C*H$_3$), 22.5, 27.5, 29.1, 31.6 (*C*H$_2$), 33.1(*C*H), 71.9, 72.0 (O*C*H$_2$CH$_2$O), 103.9 (CN), 113.5, 128.5, 136.3, 156.5 (*Ar*); IR (KBr) 2231 cm^{-1} (C≡N); MS (CI, *m*/*z*) 1029 (M$^+$,100). Anal. Calcd for $C_{64}H_{76}N_4O_8$: C, 74.68; H, 7.44; N 5.44. Found: C, 74.50; H, 7.88; N, 5.48.

8,13,18,32-Tetracyano-5,6,10,11,15,16,20,21-octahydro-1,25,27,29-tetraundecyl-2,24:3,23-dimetheno-1*H*,25*H*,27*H*,29*H*-bis[1,4]dioxonino[6,5-*j*:6′,5′-*j*′]benzo[1,2-*e*:5,4-*e*′]bis[1,4]benzodioxonin (2b). The collected solid was loaded onto the top of a silica gel flash column; elution with a mixture of methylene chloride:acetone 98:2 afforded the compound **2b** as a white solid (81% yield): mp 161−164 °C; ^{1}H NMR (300 MHz, $CDCl_3$) δ 0.87 [t, 12H, CHCH$_2$-(CH$_2$)$_9$C*H*$_3$], 1.26 [m, 72H, CHCH$_2$(C*H*$_2$)$_9$CH$_3$], 2.05 [m, 8H, CHC*H*$_2$(CH$_2$)$_9$-CH$_3$], 3.81 (m, 8H, OC*H*$_{in}$C*H*$_{in}$O), 4.59 (m, 8H, OC*H*$_{out}$C*H*$_{out}$O), 5.23 (t, 4H, C*H*C$_{11}$H$_{23}$), 7.41 (s, 4H, Ar*H*); IR (KBr) 2231 cm^{-1} (C≡N); MS (CI) *m*/*z* 1311 (MH$^+$, 100). Anal. Calcd for $C_{84}H_{116}N_4O_8$: C, 77.02; H, 8.92; N, 4.28. Found: C, 76.95; H, 9.03; N, 4.48.

Procedure for the Self-Assembly of Coordination Cages 7a−g. To a solution of cavitand **1a−c** (0.024 mmol) in 10 mL of CH_2Cl_2 was added the complex $ML_2(OTf)_2$ **3a−h/4a** (0.048 mmol), and the resulting solution was stirred at room temperature for a few minutes. The solvent was then removed under vacuum, affording the cages **7a−g** in quantitative yield.

7a. Pale yellow solid: mp 180 °C (dec); ^{1}H NMR ($CDCl_3$, 300 MHz) δ 0.84 (t, 24H, C*H*$_3$, J = 6.8 Hz), 1.29−1.25 [m, 80H, CH$_3$(C*H*$_2$)$_5$], 1.50 [bs, 16H, CHCH$_2$C*H*$_2$(CH$_2$)$_3$CH$_3$], 2.42 (bs, 8H, Ph$_2$PCH$_2$C*H*$_2$-CH$_2$PPh$_2$), partially superimposed to 2.39 [m, 16H, CHC*H*$_2$(CH$_2$)$_4$CH$_3$], 2.99 (bs, 16H, Ph$_2$PC*H*$_2$CH$_2$C*H*$_2$PPh$_2$), 4.04 (d, 8H, OC*H*$_{in}$O, J = 7.3 Hz), 4.39 (t, 8H, C*H*, J = 8.2 Hz), 6.07 (d, 8H, OC*H*$_{out}$O, J = 7.3 Hz), 7.31−7.52 (m, 80H, C$_6$*H*$_5$), 7.94 (s, 8H, Ar*H*), ^{13}C NMR ($CDCl_3$, 300 MHz) δ 14.2 (*C*H$_3$), 18.7, 22.9 [P(*C*H$_2$)$_3$P], 28.4, 28.6, 28.8, 30.1, 32.5 (*C*H$_2$), 36.9 (*C*H), 99.5 (O*C*H$_2$O), 124.5 (Ar*C*N), 125.4, 129.9, 130.0, 131.4, 132.8, 133.1, 133.4, 133.6, 133.7, 139.3, 156.9 (*Ar*); ^{31}P NMR ($CDCl_3$, 81 MHz) δ 16.7 (s); ^{19}F NMR (CD_2Cl_2, 188.3 MHz) δ −76.8 (s, 21F, $CF_3SO_3^-$ *out*), −79.9 (s, 3F, $CF_3SO_3^-$- *in*); IR (KBr) 2306 cm^{-1} (C≡N); ES-MS (acetone) *m*/*z* 2458 [M − 2$CF_3SO_3^-$]$^{2+}$, 1589 [M − 3$CF_3SO_3^-$]$^{3+}$, [M = $C_{236}H_{240}F_{24}N_8O_{40}P_8Pd_4S_8$].

7b. Pale yellow solid: mp 187 °C (dec); ^{1}H NMR ($CDCl_3$, 300 MHz) δ 0.81 (t, 24H, C*H*$_3$, J = 6.8 Hz), 1.20−1.34 [m, 128H, CH$_3$(C*H*$_2$)$_8$], 1.48 [bs, 16H, CHCH$_2$C*H*$_2$(CH$_2$)$_8$CH$_3$], 2.43 [m, 16H, CHC*H*$_2$(CH$_2$)$_9$-CH$_3$] partially superimposed to 2.55 (bs, 8H, Ph$_2$PCH$_2$C*H*$_2$CH$_2$PPh$_2$), 2.95 (bs, 16H, Ph$_2$PC*H*$_2$CH$_2$C*H*$_2$PPh$_2$), 4.03 (d, 8H, OC*H*$_{in}$O, J = 7.3 Hz), 4.38 (t, 8H, C*H*, J = 8.2 Hz), 6.07 (d, 8H, OC*H*$_{out}$O, J = 7.3 Hz), 7.21−7.60 (m, 80H, C$_6$*H*$_5$), 7.94 (s, 8H, Ar*H*); ^{13}C NMR ($CDCl_3$, 75 MHz) δ 14.0 (*C*H$_3$), 18.6, 22.6 [P(*C*H$_2$)$_3$P], 28.1, 28.4, 28.7, 29.3, 29.5, 29.6, 29.7, 30.2, 31.8 (*C*H$_2$), 36.6 (*C*H), 99.0 (O*C*H$_2$O), 116.9 (*Ar*), 121.2 (*C*F$_3$, J = 319 Hz), 124.0 (Ar*C*N), 124.9, 129.8, 131.2, 132.3, 132.7, 133.3, 138.9, 156.4 (*Ar*); ^{31}P NMR ($CDCl_3$, 81 MHz) δ 10.1 (s); ^{19}F NMR ($CDCl_3$, 188.3 MHz) δ −78.2 (21F; $CF_3SO_3^-$ *out*), −81.5 (3F; $CF_3SO_3^-$ *in*), IR (KBr) 2288 cm^{-1} (C≡N); ES-MS (acetone) *m*/*z* 2738 [M − 2CF_3SO_3]$^{2+}$, 1775 [M − 3CF_3SO_3]$^{3+}$, [M = $C_{276}H_{320}$-$F_{24}N_8O_{40}P_8Pd_4S_8$].

7c. Off-white solid: mp 245 °C dec; ^{1}H NMR ($CDCl_3$, 300 MHz) δ 0.85 (t, 24H, C*H*$_3$, J = 6.8 Hz), 1.25−1.29 [m, 80H, CH$_3$(C*H*$_2$)$_5$], 1.56 [bs, 16H, CHCH$_2$C*H*$_2$(CH$_2$)$_3$CH$_3$], 2.44 [m, 16H, CHC*H*$_2$(CH$_2$)$_4$-CH$_3$], 2.80 (bs, 8H, Ph$_2$PCH$_2$C*H*$_2$CH$_2$PPh$_2$), 3.32 (bs, 16H, Ph$_2$PC*H*$_2$-CH$_2$C*H*$_2$PPh$_2$), 4.00 (d, 8H, OC*H*$_{in}$O, J = 7.3 Hz), 4.40 (d, 8H, C*H*, J = 8.2 Hz), 6.15 (d, 8H, OC*H*$_{out}$O, J = 7.3 Hz), 7.22−7.52 (m, 80H, C$_6$*H*$_5$), 7.98 (s, 8H, Ar*H*);^{31}P NMR (CD_2Cl_2, 121 MHz) δ −13.4 ($J_{(Pt-P)}$ = 3350 Hz); ^{19}F NMR (CD_2Cl_2, 188.3 MHz) δ −77.0 (21F; $CF_3SO_3^-$ *out*), −80.0 (3F; $CF_3SO_3^-$ *in*); IR (KBr) 2306 cm^{-1} (C≡N); ES-MS (acetone) *m*/*z* 2634 [M − 2CF_3SO_3]$^{2+}$, 1706 [M − 3CF_3SO_3]$^{3+}$, [M = $C_{236}H_{240}F_{24}N_8O_{40}P_8Pt_4S_8$].

7d. Off-white solid: mp 250 °C dec; ^{1}H NMR ($CDCl_3$, 300 MHz) δ 0.82 (t, 24H, C*H*$_3$, J = 6.8 Hz), 1.20−1.26 [m, 128H, CH$_3$(C*H*$_2$)$_8$], 1.49 [bs, 16H, CHCH$_2$C*H*$_2$(CH$_2$)$_8$CH$_3$], 2.44 [m, 16H, CHC*H*$_2$(CH$_2$)$_9$-CH$_3$] partially superimposed to 2.60 (bs, 8H, Ph$_2$PCH$_2$C*H*$_2$CH$_2$PPh$_2$), 3.11 (bs, 16H, Ph$_2$PC*H*$_2$CH$_2$C*H*$_2$PPh$_2$), 3.99 (d, 8H, OC*H*$_{in}$O, J = 7.3 Hz), 4.39 (t, 8H, C*H*, J = 8.2 Hz), 6.15 (d, 8H, OC*H*$_{out}$O, J = 7.3 Hz), 7.18−7.55 (m, 80H, C$_6$*H*$_5$), 7.97 (s, 8H, Ar*H*); ^{13}C NMR ($CDCl_3$, 75 MHz) δ 13.9 (*C*H$_3$), 21.0, 21.4 [P(*C*H$_2$)$_3$P], 28.0, 28.3, 28.6, 29.1, 29.4, 29.5, 29.6, 30.0, 31.7 (*C*H$_2$), 36.5 (*C*H), 98.4 (O*C*H$_2$O), 121.2 (*C*F$_3$, J = 319 Hz), 123.8 (Ar*C*N), 129.6, 129.8, 131.8, 132.2, 132.5, 133.3, 138.8, 156.6 (*Ar*); ^{31}P NMR ($CDCl_3$, 81 MHz) δ −15.7 ($J_{(Pt-P)}$ = 3317 Hz); ^{19}F NMR ($CDCl_3$, 188.3 MHz) δ −78.1 (21F; $CF_3SO_3^-$ *out*), −81.6 (3F; $CF_3SO_3^-$ *in*); IR (KBr) 2290 cm^{-1} (C≡N); MALDI-MS *m*/*z* 5981 [M − $CF_3SO_3^-$], [M = $C_{276}H_{320}F_{24}N_8O_{40}P_8Pt_4S_8$]; ES-MS (acetone) *m*/*z* 2916 [M − 2CF_3SO_3]$^{2+}$, 1894 [M − 3CF_3SO_3]$^{3+}$.

7e. This cage can also be collected by precipitation from chloroform and filtration (off-white powder): mp 240 °C dec; ^{1}H NMR (CD_2Cl_2, 400 MHz) δ 2.58−2.65 (m, 24H, CHC*H*$_2$CH$_2$Ph and Ph$_2$PCH$_2$C*H*$_2$-CH$_2$PPh$_2$), 2.80 (m, 16H, CHCH$_2$C*H*$_2$Ph), 3.04 (bs, 16H, Ph$_2$PC*H*$_2$-CH$_2$C*H*$_2$PPh$_2$), 3.98 (d, 8H, OC*H*$_{in}$O, J = 7.4 Hz), 4.44 (t, 8H, C*H*CH$_2$CH$_2$Ph), 6.18 (d, 8H, OC*H*$_{out}$O, J = 7.4 Hz), 7.20−7.56 [m, 120H, CH$_2$C$_6$*H*$_5$ + (C$_6$*H*$_5$)$_2$P(CH$_2$)$_3$P(C$_6$*H*$_5$)$_2$], 8.09 (s, 8H, Ar*H*); ^{31}P NMR (CD_2Cl_2, 121 MHz) δ −13.9 ($J_{(Pt-P)}$ = 3400 Hz); ^{19}F NMR (CD_2Cl_2, 188.3 MHz) δ −77.8 (21F, $CF_3SO_3^-$ *out*), −80.5 (3F, $CF_3SO_3^-$ *in*); IR (KBr) 2296 cm^{-1} (C≡N); ES-MS ($CHCl_3$) *m*/*z* 2715 [M − 2$CF_3SO_3^-$]$^{2+}$, 1761 [M − 3$CF_3SO_3^-$]$^{3+}$, [M = $C_{252}H_{208}F_{24}N_8O_{40}P_8$-

Pt_4S_8]. Anal. Calcd for $C_{252}H_{208}F_{24}N_8O_{40}P_8Pt_4S_8$: C, 52.83; H, 3.66; N, 1.95. Found: C, 52.59; H, 3.83; N, 1.50.

7f. ^{1}H NMR ($C_2D_2Cl_4$, 300 MHz, 373 K) δ 0.95 (t, 24H, CH_3), 1.32−1.35 [m, 128H, $CHCH_2CH_2(CH_2)_8CH_3$], 1.52 [m, 16H, $CHCH_2CH_2$-$(CH_2)_8CH_3$], 2.46 [m, 32H, $CHCH_2(CH_2)_9CH_3$ + $Ph_2PCH_2CH_2CH_2$-CH_2PPh_2], 2.80 [m, 16H, $Ph_2PCH_2(CH_2)_2CH_2PPh_2$], 4.12 (d, 8H, OC$H_{in}$O, J = 7.4 Hz), 4.49 (t, 8H, CH), 6.40 (d, 8H, OCH_{out}O, J = 7.4 Hz), 7.47−7.65 (m, 80H, C_6H_5), 7.95 (s, 8H, ArH); ^{31}P NMR ($C_2D_2Cl_4$, 81 MHz, 373 K) δ 28.3; ^{19}F NMR ($C_2D_2Cl_4$, 188.3 MHz, 373 K) δ −76.8 (21F, $CF_3SO_3^-$ *out*), −80.5 (3F, $CF_3SO_3^-$ *in*).

7g. ^{1}H NMR ($CDCl_3$, 300 MHz, 328 K) δ 0.88 (t, 24H, CH_3), 1.27 [m, 216H, $CHCH_2(CH_2)_9CH_3$ + PCH_2CH_3], 2.07 (m, 48H, PCH_2CH_3), 2.33 [t, 16H, $CHCH_2(CH_2)_9CH_3$], 4.73 (t, 8H, CH), 4.85 (d, 8H, OCH_{in}O, J = 7.2 Hz), 5.97 (d, 8H, OCH_{out}O, J = 7.2 Hz), 7.64 (s, 8H, ArH); ^{31}P NMR ($CDCl_3$, 81 MHz, 328 K) δ 7.8 ($J_{(Pt-P)}$ = 3590 Hz); ^{19}F NMR ($CDCl_3$, 188.3 MHz, 328 K) δ −79.5 (21F, $CF_3SO_3^-$ *out*), −81.5 (3F, $CF_3SO_3^-$ *in*); ES-MS ($CHCl_3$) *m*/*z* 2558 [M − $2CF_3SO_3^-$]$^{2+}$, 1655 [M − $3CF_3SO_3^-$]$^{3+}$, [M = $C_{216}H_{324}F_{24}N_8O_{40}P_8Pt_4S_8$].

Procedure for the Self-Assembly of Coordination Cages 7h−j. To a THF solution of M(dppp)X_2 was added **5a**−**d** (M = Pd, Pt, X = BF_4, PF_6, 0.048 mmol), prepared in situ from M(dppp)Cl_2 and AgX (stoichiometric ratio 1:2) cavitand **1b** (30 mg, 0.024 mmol), dissolved in 20 mL of CH_2Cl_2, and the resulting solution was stirred at room temperature for a few minutes. The solvent was then removed under vacuum, affording cages **7h**−**j** in quantitative yield.

7h. ^{1}H NMR ($CDCl_3$, 300 MHz) δ 0.82 (t, 24H, CH_3, J = 6.9 Hz), 1.20−1.30 [m, 128H, $CH_3(CH_2)_8$], 1.49 [bs, 16H, $CHCH_2CH_2(CH_2)_8$-CH_3], 2.35 [m, 16H, $CHCH_2(CH_2)_9CH_3$] 2.54 (bs, 8H, $Ph_2PCH_2CH_2$-CH_2PPh_2), 2.94 (bs, 16H, $Ph_2PCH_2CH_2CH_2PPh_2$), 4.12 (d, 8H, OCH_{in}O, J = 7.0 Hz), 4.36 (t, 8H, CH, J = 7.9 Hz), 6.19 (d, 8H, OCH_{out}O, J = 7.0 Hz), 7.21−7.63 (m, 80H, C_6H_5), 7.84 (s, 8H, ArH); ^{31}P NMR ($CDCl_3$, 81 MHz) δ +11.1; ^{19}F NMR ($CDCl_3$, 188.3 MHz) δ −150.4 (28F, BF_4^- *out*), −151.3 (4F; BF_4^- *in*); MALDI-MS *m*/*z* 5191 [M − BF_4^-]$^+$, [M = $C_{268}H_{320}B_8F_{32}N_8O_{16}P_8Pd_4$].

7i. Yellow solid: mp 195 °C dec; ^{1}H NMR ($CDCl_3$, 300 MHz) δ 0.82 (t, 24H, CH_3, J = 6.9 Hz), 1.20−1.27 [m, 128H, $CH_3(CH_2)_8$], 1.51 [bs, 16H, $CHCH_2CH_2(CH_2)_8CH_3$], 2.37 [m, 16H, $CHCH_2(CH_2)_9$-CH_3] 2.51 (bs, 8H, $Ph_2PCH_2CH_2CH_2PPh_2$), 3.06 (bs, 16H, Ph_2PCH_2-$CH_2CH_2PPh_2$), 4.10 (d, 8H, OCH_{in}O, J = 7.0 Hz), 4.36 (t, 8H, CH, J = 7.9 Hz), 6.24 (d, 8H, OCH_{out}O, J = 7.0 Hz), 7.16−7.60 (m, 80H, C_6H_5), 7.92 (s, 8H, ArH); ^{31}P NMR (CD_2Cl_2, 81 MHz) δ −14.5 ($J_{(Pt-P)}$ = 3335 Hz); ^{19}F NMR ($CDCl_3$, 188.3 MHz) δ −150.0 (28F, BF_4^- *out*), −151.0 (4F; BF_4^- *in*); ES-MS ($CHCl_3$) *m*/*z* 2788 [M·$CHCl_3$ − $2BF_4^-$]$^{2+}$, 1830 [M·$CHCl_3$ − $3BF_4^-$]$^{3+}$, [M = $C_{268}H_{320}B_8F_{32}N_8O_{16}P_8$-$Pt_4$]; ES-MS (acetone) *m*/*z* 2758 [M·$(CH_3)_2CO$ − $2BF_4^-$]$^{2+}$, 1810 [M·$(CH_3)_2CO$ − $3BF_4^-$]$^{3+}$.

7k. This cage is unstable both in solution and in the solid state. It must be stored in the dark under an Ar atmosphere.^{1}H NMR ($CDCl_3$, 300 MHz) δ 0.84 (t, 24H, CH_3, J = 6.9 Hz), 1.20−1.25 [m, 128H, $CH_3(CH_2)_8$], 1.40 [m, 16H, $CHCH_2CH_2(CH_2)_8CH_3$], 2.35 [m, 16H, $CHCH_2(CH_2)_9CH_3$], 2.74 (bs, 8H, $Ph_2PCH_2CH_2CH_2PPh_2$), 2.92 (bs, 16H, $Ph_2PCH_2CH_2CH_2PPh_2$), 3.89 (d, 8H, OCH_{in}O, J = 7.0 Hz), 4.39 (t, 8H, C$HC_{11}H_{23}$, J = 7.6 Hz), 6.14 (d, 8H, OCH_{out}O, J = 7.0 Hz), 7.18−7.54 [m, 80H, $(C_6H_5)_2P(CH_2)_3P(C_6H_5)_2$], 7.74 (s, 8H, Ar$H$); ^{19}F NMR ($CDCl_3$, 188.3 MHz) δ −71.4 (d, 42F, $J_{(F-P)}$ = 712 Hz, PF_6^- *out*), −78.1 (d, 6F, $J_{(F-P)}$ = 712 Hz, PF_6^- *in*).

7j. This cage must be stored in the dark: mp 182 °C dec; ^{1}H NMR ($CDCl_3$, 300 MHz) δ 0.82 (t, 24H, CH_3, J = 6.9 Hz), 1.20−1.28 [m, 128H, $CH_3(CH_2)_8$], 1.51 [bs, 16H, $CHCH_2CH_2(CH_2)_8CH_3$], 2.37 [m, 16H, $CHCH_2(CH_2)_9CH_3$], 2.51 (bs, 8H, $Ph_2PCH_2CH_2CH_2PPh_2$), 3.02 (bs, 16H, $Ph_2PCH_2CH_2CH_2PPh_2$), 3.88 (d, 8H, OCH_{in}O, J = 7.0 Hz), 4.41 (t, 8H, C$HC_{11}H_{23}$, J = 7.9 Hz), 6.21 (d, 8H, OCH_{out}O, J = 7.0 Hz), 7.16−7.52 [m, 80H, $(C_6H_5)_2P(CH_2)_3P(C_6H_5)_2$], 7.80 (s, 8H, Ar$H$); ^{31}P NMR ($CD_2Cl_2$, 81 MHz) δ −141.0 (m, 8P, PF_6^-, $J_{(F-P)}$ = 712 Hz), −14.0 (s + d, 8P, dppp, $J_{(Pt-P)}$ = 3333 Hz); ^{19}F NMR ($CDCl_3$, 188.3 MHz) δ −71.8 (d, 42F, $J_{(F-P)}$ = 715 Hz, PF_6^- *out*), −78.7 (d, 6F, $J_{(F-P)}$ = 715 Hz, PF_6^- *in*); ES-MS (acetone and $CHCl_3$) *m*/*z* 2903 [M − $2PF_6^-$]$^{2+}$, 1887 [M − $3PF_6^-$]$^{3+}$, [M = $C_{268}H_{320}F_{48}N_8O_{16}P_{16}Pt_4$].

Procedure for the Self-Assembly of Coordination Cages 8a,b. To a solution of cavitand **2a,b** (0.027 mmol) in 20 mL of CH_2Cl_2 was added the complex Pt(dppp)$(OTf)_2$ **3g** (50 mg, 0.055 mmol) , and the resulting solution was stirred at room temperature for a few minutes. The solvent was then removed under vacuum, affording the cages **8a,b**.

8a. ^{1}H NMR ($C_2D_2Cl_4$, 300 MHz, 353 K) δ 0.83 (t, 24H, CH_3), 1.19 [bs, 64H, $CHCH_2(CH_2)_4CH_3$], 2.16 [m, 16H, $CHCH_2(CH_2)_4CH_3$], 2.48 (bs, 8H, $Ph_2PCH_2CH_2CH_2PPh_2$), 3.20 (bs, 16H, $Ph_2PCH_2CH_2CH_2$-PPh_2), 3.28 (m, 16H, OCH_{in}O), 4.45 (m, 16H, OCH_{out}O), 4.90 (t, 8H, CH), 7.34 (t, 16H, H_p-dppp), 7.45 (m, 32H, H_m-dppp), 7.59 (m, 32H, H_o-dppp), 7.94 (s, 8H, ArH); ^{31}P NMR ($CDCl_3$, 81 MHz, 353 K) δ −15.4 ($J_{(Pt-P)}$ = 3321 Hz); ^{19}F NMR (188.3 MHz, $C_2D_2Cl_4$, 353 K) δ −76.8 (21F, C$F_3SO_3^-$ *out*), −80.2 (3F, C$F_3SO_3^-$ *in*); IR (KBr) 2254 cm^{-1} (C≡N); ES-MS ($CHCl_3$) *m*/*z* 2692 [M − $2CF_3SO_3$]$^{2+}$, [M = $C_{244}H_{256}F_{24}N_8O_{40}P_8Pt_4S_8$].

8b. ^{1}H NMR ($C_2D_2Cl_4$, 400 MHz, 353 K) δ 0.89 (t, 24H, CH_3), 1.26−1.32 [m, 128H, $CHCH_2CH_2(CH_2)_8CH_3$], 1.42 [bs, 16H, $CHCH_2$-$CH_2(CH_2)_8CH_3$], 2.28 [m, 16H, $CHCH_2(CH_2)_9CH_3$], 2.55 (bm, 8H, $Ph_2PCH_2CH_2CH_2PPh_2$), 3.20 (bs, 16H, $Ph_2PCH_2CH_2CH_2PPh_2$), 3.34 (m, 16H, OCH_{in}CH_{in}O), 4.52 (m, 16H, OCH_{out}CH_{out}O), 4.95 (t, 8H, CH), 7.37 (t, 16H, H_p-dppp), 7.47 (m, 32H, H_m-dppp), 7.66 (m, 32H, H_o-dppp), 8.07 (s, 8H, ArH);^{31}P NMR ($C_2D_2Cl_4$, 81 MHz, 353 K) δ −16.1 ($J_{(Pt-P)}$ = 3337 Hz);^{19}F NMR ($C_2D_2Cl_4$, 188.3 MHz, 353 K) δ −76.8 (21F, C$F_3SO_3^-$ *out*), −80.2 (3F, C$F_3SO_3^-$ *in*); IR (KBr) 2254 cm^{-1} (C≡N); MALDI-MS *m*/*z* 6092 [M − CF_3SO_3−]$^+$ [M = $C_{284}H_{336}F_{24}N_8O_{40}P_8Pt_4S_8$]; ES-MS ($CHCl_3$) *m*/*z* 2972 [M − $2CF_3SO_3$]$^{2+}$.

Procedure for the Self-Assembly of Coordination Cages 8c,d. To a THF solution of Pt(dppp)X_2 **5b**/**5d** (X = BF_4, PF_6, 0.055 mmol), prepared in situ from Pt(dppp)Cl_2 and AgX (stoichiometric ratio 1:2), was added cavitand **2b** (35 mg, 0.027 mmol), dissolved in 20 mL of CH_2Cl_2, and the resulting solution was stirred at room temperature for a few minutes. The solvent was then removed under vacuum, affording cages **8c,d**.

8c. ^{1}H NMR ($C_2D_2Cl_4$, 400 MHz, 353 K) δ 0.82 (t, 24H, CH_3), 1.18 [bs, 128H, $CHCH_2CH_2(CH_2)_8CH_3$], 1.40 [bm, 16H, $CHCH_2CH_2$-$(CH_2)_8CH_3$], 2.24 [m, 16H, $CHCH_2(CH_2)_9CH_3$], 2.81 (bs, 8H, $Ph_2PCH_2CH_2CH_2PPh_2$), 3.14 (bs, 16H, $Ph_2PCH_2CH_2CH_2PPh_2$), 3.45 (m, 16H, OCH_{in}CH_{in}O) 4.49 (m, 16H, OCH_{out}CH_{out}O), 4.83(t, 8H, C$HC_{11}H_{23}$), 7.32 (m, 16H, H_p-dppp), 7.47 (m, 32H, H_m-dppp), 7.65 (m, 32H, H_o-dppp), 8.14 (s, 8H, ArH); ^{31}P NMR ($C_2D_2Cl_4$, 81 MHz, 353 K) δ −13.1 ($J_{(Pt-P)}$ = 3320 Hz);^{19}F NMR ($C_2D_2Cl_4$, 188.3 MHz, 353 K) δ −145.0 (4F, BF_4^- *in*), −149.1 (28F; BF_4^- *out*); ES-MS ($CHCl_3$) *m*/*z* 2845 [M·$CHCl_3$ − $2BF_4^-$]$^{2+}$, 1868 [M·$CHCl_3$ − $3BF_4^-$]$^{3+}$, [M = $C_{284}H_{336}B_8$-$F_{32}N_8O_{16}P_8Pt_4$].

8d. ^{1}H NMR ($C_2D_2Cl_4$, 400 MHz, 353 K) δ 0.83 (t, 24H, CH_3), 1.07−1.41 (m, 128H, [$CHCH_2CH_2(CH_2)_8CH_3$], 1.73 [bs, 16H, $CHCH_2CH_2(CH_2)_8CH_3$], 2.21 [m, 16H, $CHCH_2(CH_2)_9CH_3$] 2.88 (bs, 8H, $Ph_2PCH_2CH_2CH_2PPh_2$), 3.07 (bs, 16H, $Ph_2PCH_2CH_2CH_2PPh_2$), 3.20 (m, 16H, OCH_{in}CH_{in}O), 4.42 (m, 16H, OCH_{out}CH_{out}O), 4.84 (t, 8H, C$HC_{11}H_{23}$), 7.32 (m, 16H, H_p-dppp), 7.47 (m, 32H, H_m-dppp), 7.65 (m, 32H, H_o-dppp), 7.94 (s, 8H, ArH); ^{31}P NMR ($C_2D_2Cl_4$, 81 MHz, 333 K) δ − 141.0 (m, 8P, PF_6^-, $J_{(F-P)}$ = 715 Hz), −9.3 (s + d, 8P, dppp, $J_{(Pt-P)}$ = 3350 Hz); ^{19}F NMR ($C_2D_2Cl_4$, 188.3 MHz, 333 K) δ −71.7 (d, 42F, PF_6^- *out*), −76.5 (d, 6F, PF_6^- *in*). ES-MS ($CHCl_3$) *m*/*z* 2959 [M − $2PF_6^-$]$^{2+}$, 1924 [M − $3PF_6^-$]$^{3+}$, [M = $C_{284}H_{336}F_{48}N_8O_{16}P_{16}$-$Pt_4$].

Self-Assembly of Coordination Cage 10. To a solution of cavitand **9** (0.02 mmol) in 10 mL of CH_2Cl_2 was added the complex Pt(dppp)-$(OTf)_2$ **3g** (0.06 mmol), and the resulting solution was stirred at room temperature for a few minutes. The solvent was then removed under vacuum, affording cage **10** in quantitative yield.

10: mp 125 °C; ^{1}H NMR ($CDCl_3$, 300 MHz) δ 0.83 (t, 24H, CH_3), 1.22−1.24 [m, 128H, $CHCH_2CH_2(CH_2)_8CH_3$], 1.45 [bs, 16H, $CHCH_2$-$CH_2(CH_2)_8CH_3$], 2.27−2.42 [m, 16H, $CHCH_2(CH_2)_9CH_3$], superimposed to 2.64 (m, 6H, $Ph_2PCH_2CH_2CH_2PPh_2$), 3.17 (bs, 12H, Ph_2PCH_2-$CH_2CH_2PPh_2$), 3.99 (d, 4H, CH_{in}, J = 6.7 Hz), 4.27 (d, 4H, OCH_{in}O, J = 7.2 Hz), 4.42 (t, 4H, CH), 4.50 (t, 4H, CH), 5.81 (d, 4H, OCH_{out}O, J = 6.7 Hz), 6.12 (d, 4H, OCH_{out}O, J = 7.2 Hz), 6.35 (s, 2H, ArH_a), 7.05 (s, 2H, ArH_b), 7.18−7.58 (m, 60H, C_6H_5), 7.79 (s, 6H, ArH_c); ^{13}C NMR ($CDCl_3$, 75 MHz) δ 14.1 (*C*H_3), 18.5, 22.7 [$Ph_2P(CH_2)_3$-PPh_2], 28.2, 28.3, 28.8, 29.0, 29.3, 29.7, 29.8, 30.0, 30.2, 31.9 (*C*H_2), 36.4, 36.5 (*C*H), 98.2, 99.3 (O*C*H_2O), 123.1, 123.3 (Ar*C*N), 129.1, 129.3, 129.4, 129.5, 129.7, 129.9, 131.3, 131.6, 131.9, 132.4, 132.7, 132.8, 133.1, 133.2, 133.3, 137.7, 137.8, 138.5, 140.1, 154.5, 156.6,

157.8 (Ar); ^{31}P NMR ($CDCl_3$, 81 MHz) δ −16.6 ($J_{(Pt-P)}$ = 3340 Hz); ^{19}F NMR ($CDCl_3$, 188.3 MHz) δ −78.4 (18F, $CF_3SO_3^-$ *out* only); IR (KBr) 2283, 2295 cm^{-1} (C≡N).

Ligand Exchange Experiments. 1-Pd Cage: cage **7b** (29 mg, 0.005 mmol) was dissolved in 1 mL of $CDCl_3$. To this solution was added cavitand **1c** (11 mg, 0.01 mmol) dissolved in 1 mL of $CDCl_3$ stepwise. The ^{1}H NMR spectrum clearly showed five different species (see Supporting Information): cage **7b** (R = R^I = $C_{11}H_{23}$), heterocage **11** (R = $C_{11}H_{23}$, R^I = $CH_2CH_2C_6H_5$), cage **12** (R = R^I = $CH_2CH_2C_6H_5$), cavitand **1b** (R = $C_{11}H_{23}$), cavitand **1c** (R = $CH_2CH_2C_6H_5$).

^{1}H NMR ($CDCl_3$, 400 MHz, diagnostic peaks only) δ 3.92, 4.07 (d, OC*H*$_{in}$O of **11**), 3.98 (d, OC*H*$_{in}$O of **12**), 4.02 (d, OC*H*$_{in}$O of **7b**), 4.37−4.40 (t, C*H* of **7b** **11**, **12**), 4.59 (d, OC*H*$_{in}$O of **1b**), 4.61 (d, OC*H*$_{in}$O of **1c**), 4.80 (t, C*H* of **1b**), 4.90 (t, C*H* of **1c**), 7.44 (s, Ar*H* of **1c**), 7.94 (s, Ar*H* of **7b**), 7.96, 8.06 (s, Ar*H* of **11**), 8.08 (s, Ar*H* of **12**).

ES-MS ($CDCl_3$) of the mixture: *m*/*z* 2738 [**7b** − $2CF_3SO_3]^{2+}$, 2602 [**11** − $2CF_3SO_3]^{2+}$, 2538 [**12** − $2CF_3SO_3]^{2+}$.

Ligand Exchange Experiments. 2-Pt cage: cage **7d** (31 mg, 0.005 mmol) was dissolved in 1 mL of $CDCl_3$. To this solution was added cavitand **1c** (11 mg, 0.01 mmol) dissolved in 1 mL of $CDCl_3$ stepwise. Immediately after the addition at 300 K, no ligand exchange was observed. Equilibration was reached after 4 h. The same experiment was repeated at 330 K, giving immediate ligand exchange.

The following compounds were detected via ^{1}H NMR: cage **7d** (R = R^I = $C_{11}H_{23}$), heterocage **13** (R = $C_{11}H_{23}$, R^I = $CH_2CH_2C_6H_5$), cage **7e** (R = R^I = $CH_2CH_2C_6H_5$), cavitand **1b** (R = $C_{11}H_{23}$), cavitand **1c** (R = $CH_2CH_2C_6H_5$).

^{1}H NMR ($CDCl_3$, 400 MHz, 330 K) δ 3.94−4.05 (d, OC*H*$_{in}$O of **7d**, **7e**, **13**), 4.39−4.45 (t, C*H* di **7d**, **7e**, **13**), 4.59 (d, OC*H*$_{in}$O of **1b**), 4.62 (d, OC*H*$_{in}$O of **1c**), 4.82 (t, C*H* of **1b**), 4.89 (t, C*H* of **1c**), 7.45 (s, Ar*H* of **1c**), 8.02 (s, Ar*H* of **7d**), 8.02, 8.14 (s, Ar*H* of **13**), 8.16 (s, Ar*H* of **7e**).

After standing a few days, a white solid precipitated from the solution. It was collected and dissolved in CD_2Cl_2. Its ^{1}H NMR spectrum was superimposable on that of pure **7e**.

ES-MS ($CDCl_3$) of the mixture: *m*/*z* 2916 [**7d** − $2CF_3SO_3]^{2+}$, 2780 [**13** − $2CF_3SO_3]^{2+}$, 2715 [**7e** − $2CF_3SO_3]^{2+}$.

X-ray Structural Analysis of Cage 7d. A suitable colorless crystal (0.4 × 0.3 × 0.2 mm) of $2[C_{134}H_{160}N_4O_8P_4Pt_2]^{4+}\cdot 8CF_3SO_3^-\cdot 12.5C_6H_6$ was obtained from dichloromethane−benzene, M = 7106.50, triclinic *P*-1, a = 21.1806(4), b = 28.9684(7), and c = 29.2633(7) Å, α = 81.8122(12), β = 74.7096(12), and γ = 85.3796(12)°, V = 17 125.5(7) Å^3, μ(Mo Kα) = 1.791 mm^{-1} (based on found atoms, see below), Z = 2, D_c = 1.308 g cm^{-3}, F(000) = 6860, T = 173.0(1) K. Data were recorded with a Nonius Kappa CCD diffractometer, using 396 frames, each frame covering a 1° oscillation with an exposure time of 2 × 20 s. A total of 112391 collected reflections and 77319 unique reflections [30704 $I > 2\sigma(I)$] were used for refinement. The data were processed with Denzo.[34] The absorption correction was made with SORTAV (Blessing, R. H. *Acta Crystallogr*. **1995**, *A51*, 33−37,), but not applied. L_p correction was applied. Structure solution was done by direct methods[35] and refinement on F^2.[36] The hydrogen atoms were calculated to their idealized positions with isotropic temperature factors (1.2 or 1.5 times the C temperature factor) and were refined as riding atoms. A total of 34 hydrogen atoms could not be calculated to the located alkyl groups. In addition, 17 alkylic carbon atoms and their H atoms could not be located. A total of 78 geometrical DFIX restraints were needed to make some of the alkyl chains and three triflate anions chemically reasonable. The phenyl groups of the Pt-cage and the benzene solvent molecules were constrained to the regular hexagons. One of the phenyl groups of the Pt-cage is disordered between two positions with site occupation values of 0.5. Altogether five temperature factors were equalized. One triflate is disordered (occupancy 0.5) over two orientations and is included into cavity of the Pt-cage. Their temperature factors were fixed to 0.25. The final R values were R = 0.1115, wR^2 = 0.2485 [$I > 2\sigma(I)$], R = 0.2684, wR^2 = 0.3164 (all data) for 2438 parameters, Goodness-of-fit on F^2 = 1.017. A final difference map displayed the highest electron density of 2.51 e Å^{-3}, which is located near to Pt-atoms and triflate anions. The crystallographic data have been deposited with the Cambridge Crystallographic Data Centre as supplementary publication no. CCDC 128551. The crystals are stable only in the presence of solvent and are destroyed upon exposure to air within seconds. The selected crystal was placed with loop in oil.

ES-MS Experiments: Electrospray mass spectra were obtained using a triple quadrupole Perkin-Elmer API 365 SCIEX spectrometer with an ionspray interface (mass range <3000 amu). The sample were introduced at a flow rate of 0.5 mL/h; the ion spray, orifice and ring potentials were set to 5500, 30, and 400 V, respectively. The scan range was set to 1500−3000 uma, accumulating 10 scans for each experiment.

MALDI-TOF Mass Spectra. MALDI-TOF mass spectra were recorded on a PerSpective Biosystem Voyager-DE-RP spectrometer equipped with delayed extraction.[37] A 337 nm UV nitrogen laser producing 3 ns pulses was used, and the mass spectra were obtained in the linear and reflectron mode. The samples were prepared by mixing 10 μL of a chloroform solution of the cage with 30 μL of a solution of 1 mg/L hydroxybenzylidene malononitrile [HBM] in chloroform/poly(ethylene glycol). One microliter of the solution was loaded on a gold-sample plate, the solvent was removed in warm air, and the sample was transferred to the vacuum of the mass spectrometer for analysis.

Calorimetric Measurements. Reaction heats were measured by means of a Thermometric Thermo Activity Monitor Microcalorimeter equipped with a flow-mixing cell (steady-state experiments) by mixing a freshly prepared 1 mM solution of Pt(dppp)$(OTf)_2$ **3g** in tetrachloroethane with a 0.5 mM solution of either **1b** or **2b** in the same solvent at 298 and 343 K, respectively. The solutions were thermostated at the experience temperature by means of a Heto cryothermostatic bath and then injected in the cell of the calorimeter by means of a Gilson peristaltic pump, Minipuls 2, equipped with Viton tubing (internal diameter 1.5 mm) at a flow rate of 5 × 10^{-3} g s^{-1}. Heats of reaction were experimentally corrected for the heats of dilution of both reactant solutions. The reported values are the average of at least four different measurements.

Acknowledgment. The paper is dedicated to the memory of Don Cram. This work was supported by CNR (Nanotechnology Program) and MURST (Molecular Nanoelectronics Project). Use was made of instrumental facilities at the Centro Interfacoltà di Misure G. Casnati of the University of Parma. Financial support from INSTM to P.J. and from the Finnish Ministry of Education to E.W. is gratefully acknowledged. Finally, we are grateful to Prof. J. C. Sherman (UBC) for helpful suggestions.

Supporting Information Available: Experimental procedures and characterization of tetrabromo cavitand precursors of compounds **2a,b**, metal complexes **3a**−**h**, **4a**, **5a**−**d**, and **6a**−**d**; MALDI-TOF spectrum of cage **7d**; FT-IR monitoring of CSA; X-ray structural information on **7d**. This material is available free of charge via the Internet at http://pubs.acs.org.

JA0103492

(34) Otwinowski, Z.; Minor, W. *Methods in Enzymology*; Carter, C. W., Jr., Sweet, R. M., Eds.; Academic Press: New York, 1997; Vol. 276, Macromolecular Crystallography, part A, pp 307−326.

(35) Sheldrick, G. M. *SHELXS97 − A Program for Automatic Solution of Crystal Structures*; University of Göttingen: Germany, 1997.

(36) Sheldrick, G. M. *SHELXL97 − A Program for Crystal Structure Refinement*; University of Göttingen: Germany, 1997.

(37) (a) Karas, M.; Bachmann, D.; Bahr, U.; Hillenkamp, F. *Int. J. Mass Spectrom. Ion Process.* **1987**, *78*, 53−68. (b) Vestal, M. L.; Juhasz, P.; Martin, S. A. *Rapid Commun. Mass Spectrom.* **1995**, *9*, 1044−1050.